

The 2D evolution of Nova from the onset of convection to outburst

Kavli Institute - March 15 2007

Ami Glasner , Eli Livne

The Hebrew University, Jerusalem

&

Jim Truran

The University of Chicago

Former results



Semianalytical models & Dimensional considerations



- Shara (ApJ 243,926; 1982)
“Volcanic” localized eruptions → early perturbations ?
- Fryxell & Woosley (ApJ 261,332; 1982)

Dimensional analysis of multidimensional effects for TNRs that occur on thin stellar shells.

Claim that for the Nova case there is initiation at a point and a flame that spreads by small scale turbulence with velocity:

$$V = (h_p v_c / \tau_b)^{1/2}$$

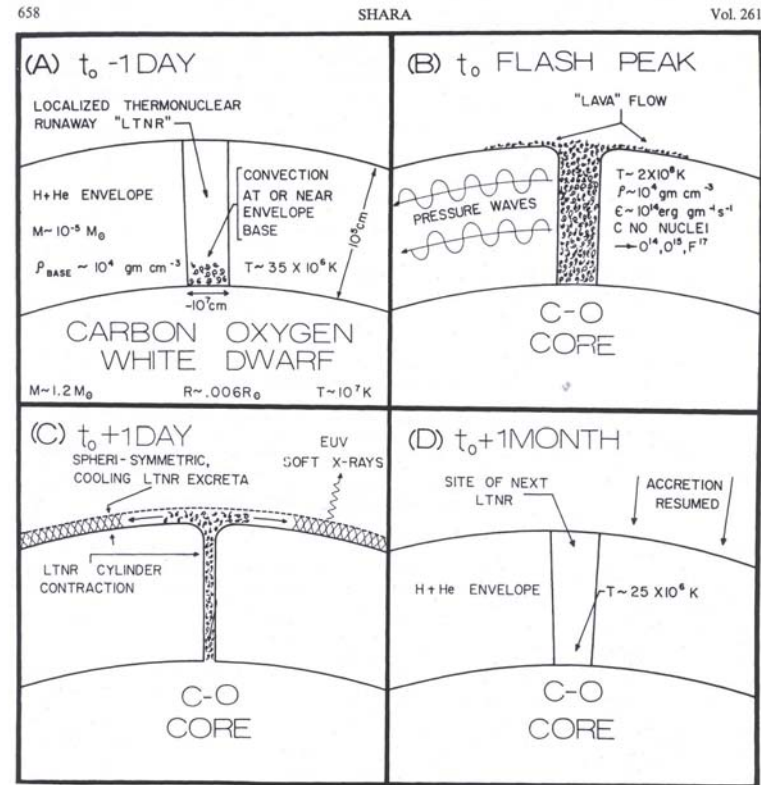
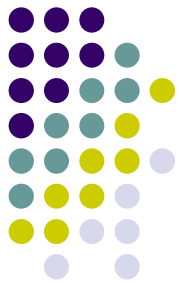


FIG. 3.—A series of qualitative sketches of the likely hydrodynamical behavior of the matter in a localized thermonuclear runaway on a white dwarf. Details are given in the text of § VI.

Who ?

How ?



Shankar, Arnett & Fryxell

PPM

(ApJ 394,L13; 1992)

(ApJ 433,216; 1994)

Kereek, Hillebrandt & Truran

PPM

2D (A&A 337,379; 1998)

3D (A&A,345,831; 1999)

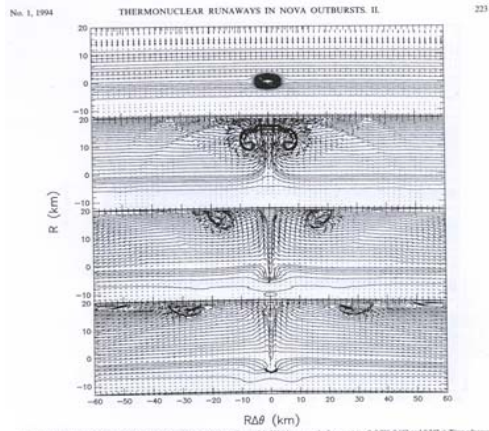
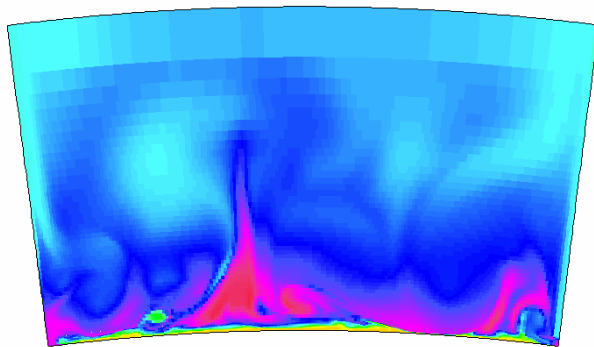
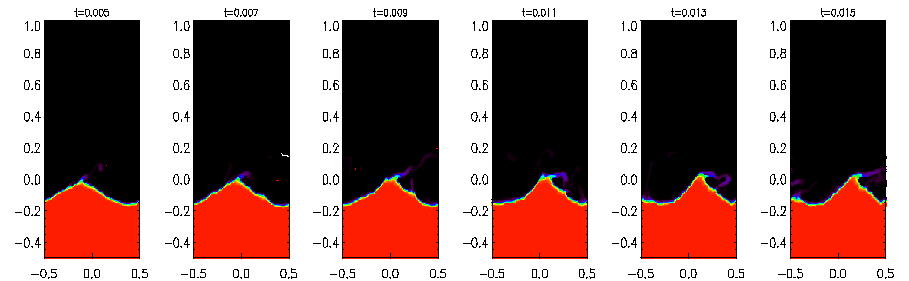
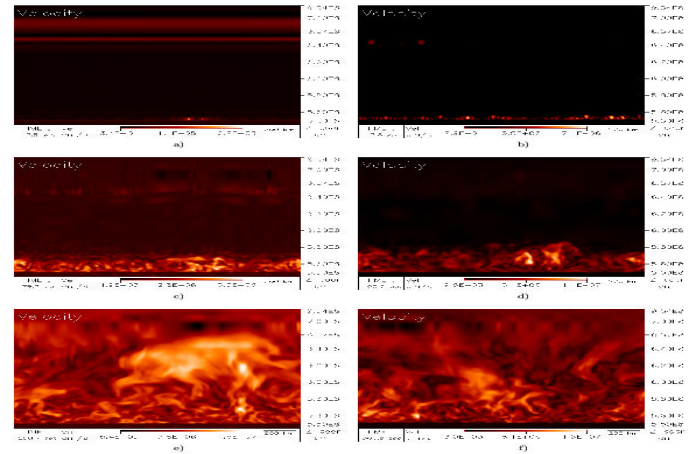


Fig. 1.—Time evolution of the velocity field and temperature contours for model M1 (shown on the frames at $t = 0.006, 0.102$ and 0.247 in Time above).
downward.



Glaser, Livne & Truran ALE

(ApJ,445,L149; 1995) (ApJ,475,754; 1997)



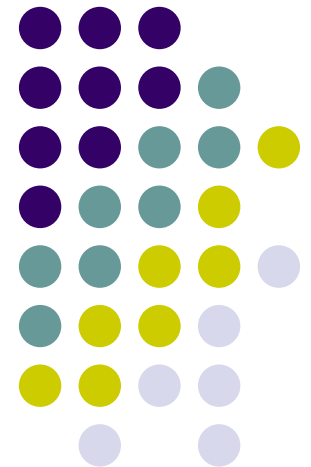
Flash PPM

Alexakis,A., Young,Y.-N. and Rosner,R. 2002,*Phys.Rev.E*,
65,026313.

Alexakis,A., Calder,A.C., Heger,A., Brown,E.F., Dursi,L.J.,
Truran,J.W., Rosner,R., Lamb,D.Q., Timmes,F.X., Fryxell,B.,
Zingales,M., Ricker,P.M., & Olson,K. 2004, ApJ, 602, 931

The main Issue:

The reliability of the mixing results ?



Abundances - Observations



ON THE FREQUENCY OF OCCURRENCE OF OXYGEN-NEON-MAGNESIUM WHITE DWARFS IN CLASSICAL NOVA SYSTEMS

JAMES W. TRURAN AND MARIO LIVIO¹

Department of Astronomy, University of Illinois

Received 1985 October 31; accepted 1986 March 4

TABLE 2

HEAVY-ELEMENT ABUNDANCES IN NOVAE

OBJECT	DATE	REFERENCE	MASS FRACTIONS											
			H	He	C	N	O	Ne	Na	Mg	Al	Si	S	Fe
RR Pic	1925	1	0.53	0.43	0.0039	0.022	0.0058	0.011
HR Del	1967	2	0.45	0.48	...	0.027	0.047	0.0030
T Aur	1891	3	0.47	0.40	...	0.079	0.051
V1500 Cyg	1975	4	0.49	0.21	0.070	0.075	0.13	0.023
V1668 Cyg	1978	5	0.45	0.23	0.047	0.14	0.13	0.0068
V693 Cr A	1981	6	0.29	0.32	0.0046	0.080	0.12	0.17	0.0016	0.0076	0.0043	0.0022
DQ Her	1934	7	0.34	0.095	0.045	0.23	0.29
V1370 Aql	1982	8	0.053	0.085	0.031	0.095	0.061	0.47	...	0.0092	...	0.0012	0.19	0.0059

REFERENCES.—(1) Williams and Gallagher 1979. (2) Tylenda 1978. (3) Gallagher *et al.* 1980. (4) Ferland and Shields (1978). (5) Stickland *et al.* 1981. (6) Williams *et al.* (1985). (7) Williams *et al.* 1978. (8) Snijders *et al.* 1984.

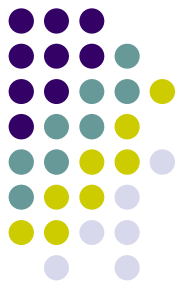


TABLE 1
HELIUM ABUNDANCES IN NOVAE

Nova	Date	HE/H	Z	Reference	Enriched Fraction
T Aur	1891	0.21	0.13	1	0.36
RR Pic	1925	0.20	0.039	2	0.28
DQ Her	1934	0.08	0.56	2	0.55
CP Lac	1936	0.11 ± 0.02	...	2	0.08
RR Tel	1946	0.19	...	2	0.24
DK Lac	1950	0.22 ± 0.04	...	2	0.30
V446 Her	1960	0.19 ± 0.03	...	2	0.24
V533 Her	1963	0.18 ± 0.03	...	2	0.23
HR Del	1967	0.23 ± 0.05	0.077	2	0.35
V1500 Cyg	1975	0.11 ± 0.01	0.30	2	0.34
V1668 Cyg	1978	0.12	0.32	3	0.38
V693 Cr A	1981	0.28	0.38	4	0.61
V1370 Aql	1982	0.40	0.86	5	0.93

REFERENCES.—(1) Gallagher *et al.* 1980. (2) Ferland 1979. (3) Stickland *et al.* 1981. (4) Williams *et al.* 1985; Williams 1985. (5) Snijders *et al.* 1984.



ABUNDANCE ANALYSIS OF THE EXTREMELY FAST ONeMg NOVAE V838 HERCULIS AND V4160 SAGITTARI

GREG J. SCHWARZ

Department of Geology and Astronomy, West Chester University, West Chester, PA; gschwarz@as.arizona.edu

STEVEN N. SHORE

Dipartimento di Fisica “Enrico Fermi,” Università di Pisa, I-56127 Pisa, Italy; INFN-Sezione di Pisa; shore@df.unipi.it

SUMNER STARRFIELD

School of Earth and Space Exploration, Arizona State University, Tempe, AZ; sumner.starfield@asu.edu

AND

KAREN M. VANLANDINGHAM

Department of Geology and Astronomy, West Chester University, West Chester, PA; kvanlandingham@wcupa.edu

Received 2006 April 26; accepted 2006 November 6

462

SCHWARZ ET AL.

Vol. 657

TABLE 6
 MASS FRACTION COMPARISON OF FIVE RECENTLY MODELED ONeMg NOVAE

Element ^a	QU Vul	V1974 Cyg	V382 Vel	V4160 Sgr	V838 Her	Solar
H.....	6.27E-01	5.52E-01	6.61E-01	4.65E-01	5.62E-01	7.02E-01
He.....	3.01E-01	2.65E-01	2.64E-01	3.34E-01	3.14E-01	2.80E-01
C.....	5.34E-04	1.64E-03	1.69E-03	6.44E-03	1.24E-02	2.99E-03
N.....	9.83E-03	3.24E-02	1.46E-02	5.77E-02	1.79E-02	9.17E-04
O.....	1.85E-02	8.51E-02	2.66E-02	6.06E-02	7.99E-03	8.31E-03
Ne.....	3.21E-02	5.47E-02	2.65E-02	6.47E-02	6.96E-02	1.65E-03
Mg.....	5.79E-03	2.34E-03	1.58E-03	4.29E-03	6.74E-04	6.48E-04
Al.....	2.66E-03	>4.39E-05	1.10E-03	...	1.02E-03	5.58E-05
Si.....	1.24E-03	5.50E-04	3.29E-04	4.90E-03	3.52E-03	6.99E-04
S.....	8.14E-03	3.64E-04
Ar.....	2.79E-05	1.11E-04
Fe.....	6.01E-04	4.99E-03	...	8.41E-04	1.42E-03	1.27E-03
Z.....	7.17E-02	1.82E-01	7.42E-02	1.99E-01	1.22E-01	1.70E-02
CNO.....	2.9E-02	1.19E-01	4.3E-02	1.25E-01	3.8E-02	1.2E-02
O/N.....	1.9E-00	2.6E-00	1.8E-00	1.0E-00	4.0E-01	9.1E-00
O/C.....	3.46E+01	5.19E+01	1.57E+01	9.4E-00	6.4E-01	2.7E-00

NOTE.—Where the H + He + Z = 1.

^a Solar values were assumed for elements that did not have reported abundances.

Mixing Mechanisms



Mixing

→ mechanisms

→ effect on burning and nucleosynthesis



Mechanisms:

- **Diffusion**

(Prialnik and Kovetz, Iben Fujimoto and MacDonald)

- **Shear induced mixing**

(Kippenhan&Thomas, MacDonald, The flash team-Chicago)

- **Undershoot of convective flows**

(Woosely, Glasner Livne&Truran, Kercek Hillebrandt & Truran)

Diffusion



- Takes place on the longest time scales (accretion).
- Mixing once the envelope becomes unstable to convection.
- The amount of mixing depends on the accretion rate.
- Z enrichment in simulations $\sim Z$ observed.



PRIALNIK AND KOVETZ

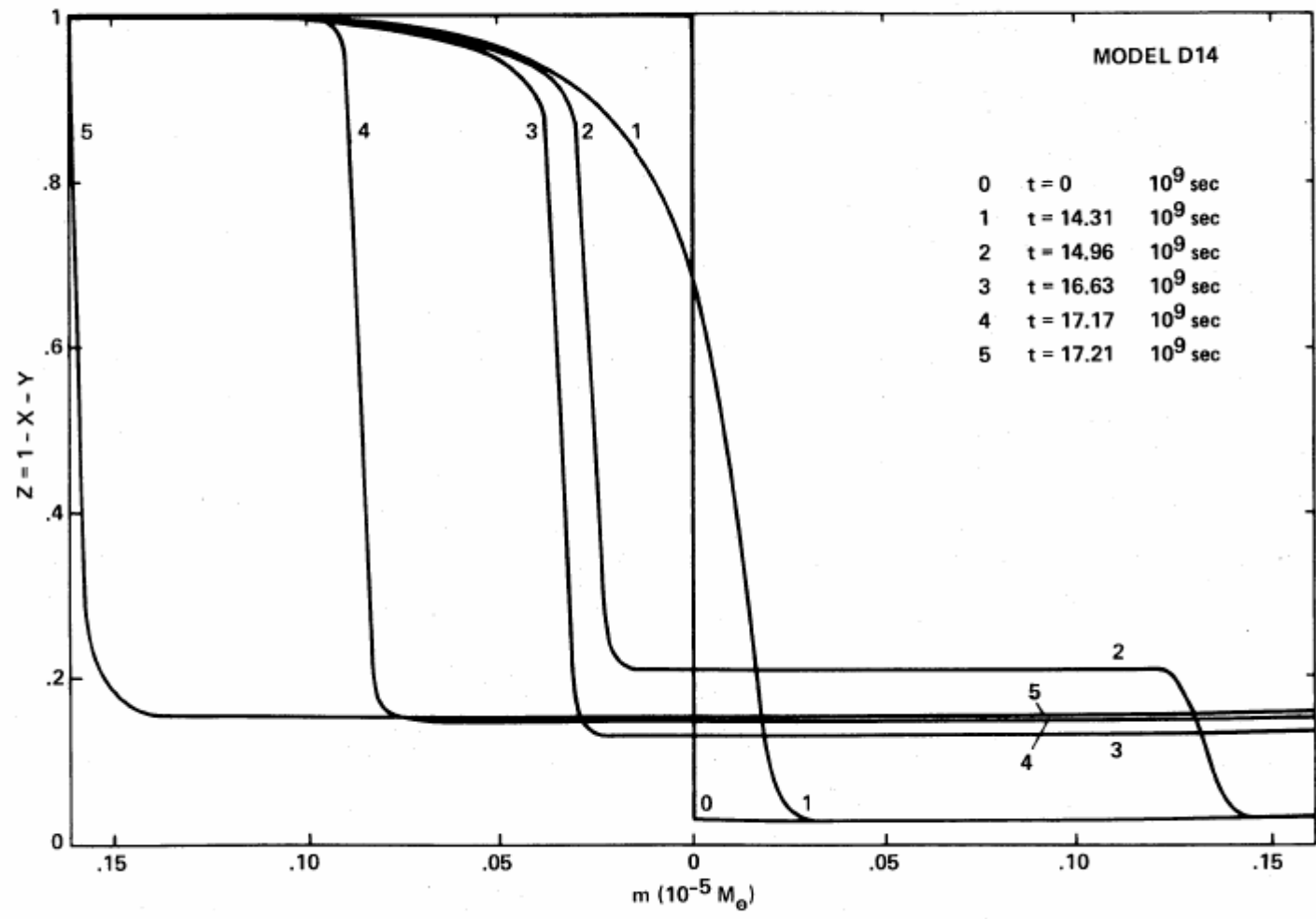


FIG. 2.—Heavy-element (Z) profiles for D14 at different times. Mass scale as in Fig. 1.

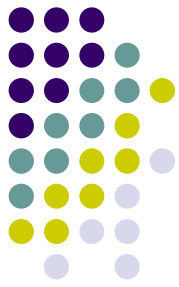
All the mixing takes place prior to the runaway !

shear



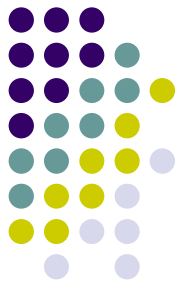
- Shear Instability in the stratified boundary between the core and the accreted envelope associated with the accretion disk.
- Resonant interaction of the shear flow with gravity (ocean) waves in the core.
- Very early creation of boundary mixed layer
- Mixing once the envelope becomes unstable to convection.

Convective undershoot Mixing



The New Models

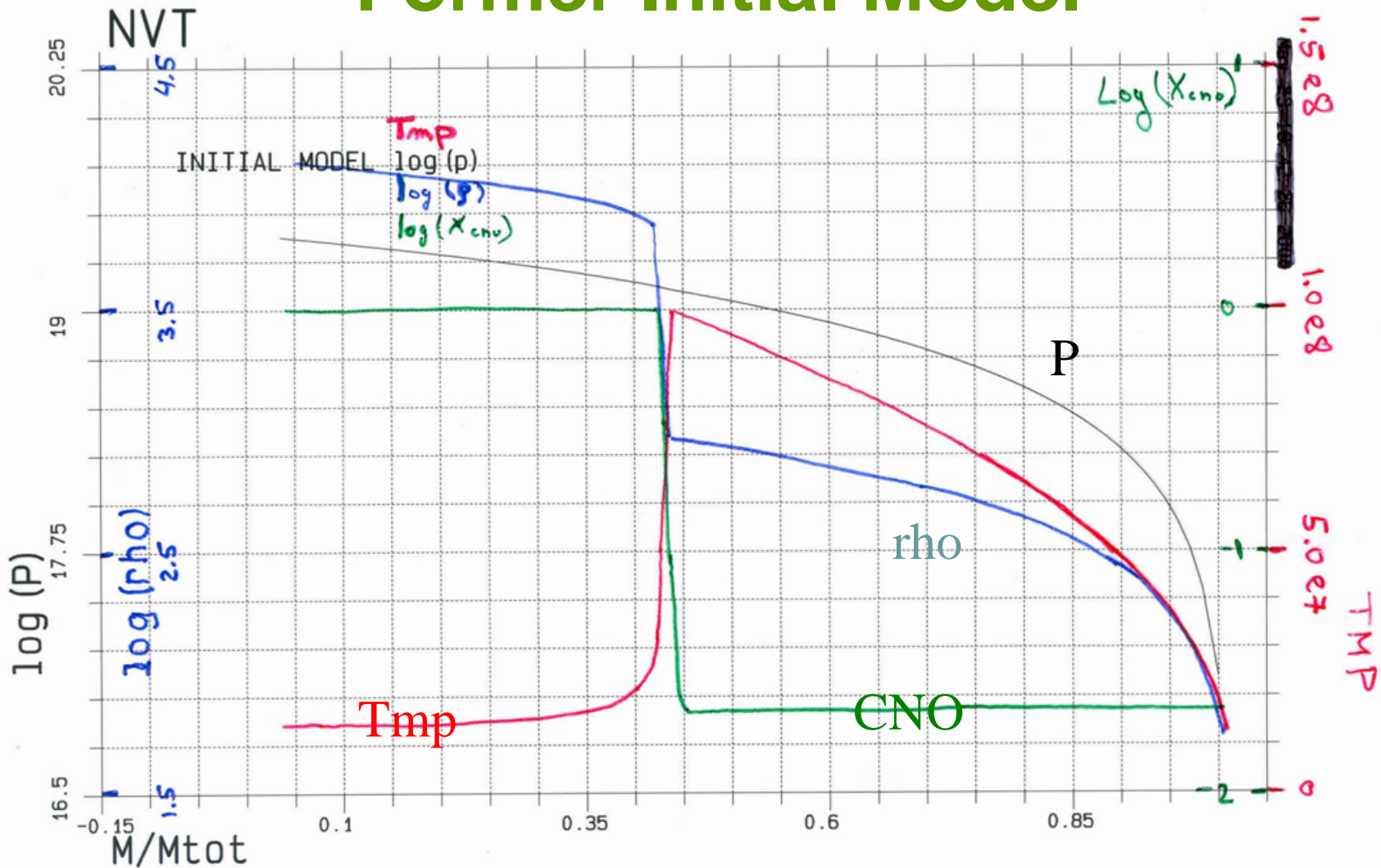




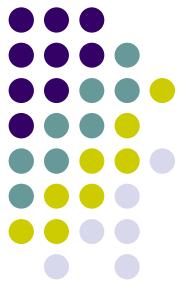
Why do we need more work ?

- Initial model at earlier stages → close to the onset of convection
- The evolution of early perturbations
- Resolution –
 - a) KH limit on wave length: $k \gtrsim g / U_{\max}^2 (1 - \rho_1 / \rho_2)$
 $U_{\max} \sim 100 \text{ km/sec}$; $g \sim 5 \cdot 10^8 \text{ cm/sec}^2$
 $k \sim 10^{(-6)}$ → wavelength $\sim 10^6 \text{ cm}$
 - b) numerical convergence
- Improving the numerical schemes

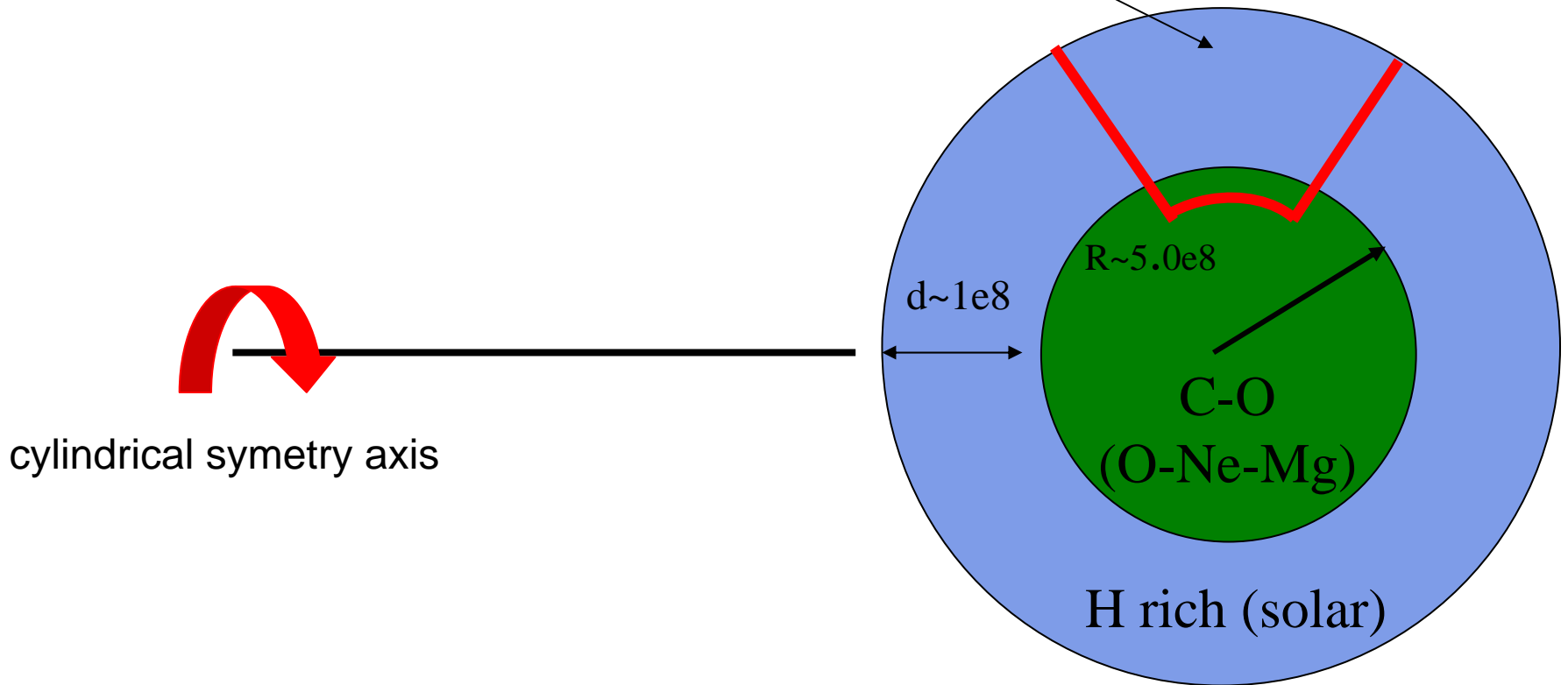
Former Initial Model

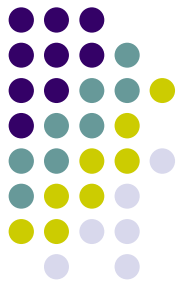


- Steep gradients at the base of the envelope
- Base Temperature of $10 \cdot 10^7$ Deg
- In 1D unstable to convection at $T_{base} \sim 3e7$ Deg



The Simulated part of the star





The initial model consists of a $1.14 M_{\odot}$ CO white dwarf in hydrostatic and thermal equilibrium, cooled to the stage at which the luminosity of the WD is about $1.6 \times 10^{-2} L_{\odot}$. Using a 1D hydro-evolution code (Glasner & Truran 2007), matter with solar abundances (Anders & Grevesse 1989) is accreted onto the surface of the CO core continuously at a rate of $1.0 \times 10^{-9} M_{\odot} \text{ yr}^{-1}$. The elements included in our reaction net are : ${}^1\text{H}, {}^3\text{He}, {}^4\text{He}, {}^7\text{Be}, {}^8\text{B}, {}^{12}\text{C}, {}^{13}\text{C}, {}^{13}\text{N}, {}^{14}\text{N}, {}^{15}\text{N}, {}^{14}\text{O}, {}^{15}\text{O}, {}^{16}\text{O}, {}^{17}\text{O}, {}^{17}\text{F}$. Diffusion and mixing of the chemical elements between the accreted envelope and the core are not included in the 1D code. The total amount of accreted matter at the time of runaway is $3.5 \times 10^{-5} M_{\odot}$.

grid: $1.4\text{km} \times 1.4\text{km}$

Typical values are:

$$V_{\text{early-convection}} \approx 50 \text{ Km/sec}$$

where $V_{\text{early-convection}}$ is the typical local early convective velocity.

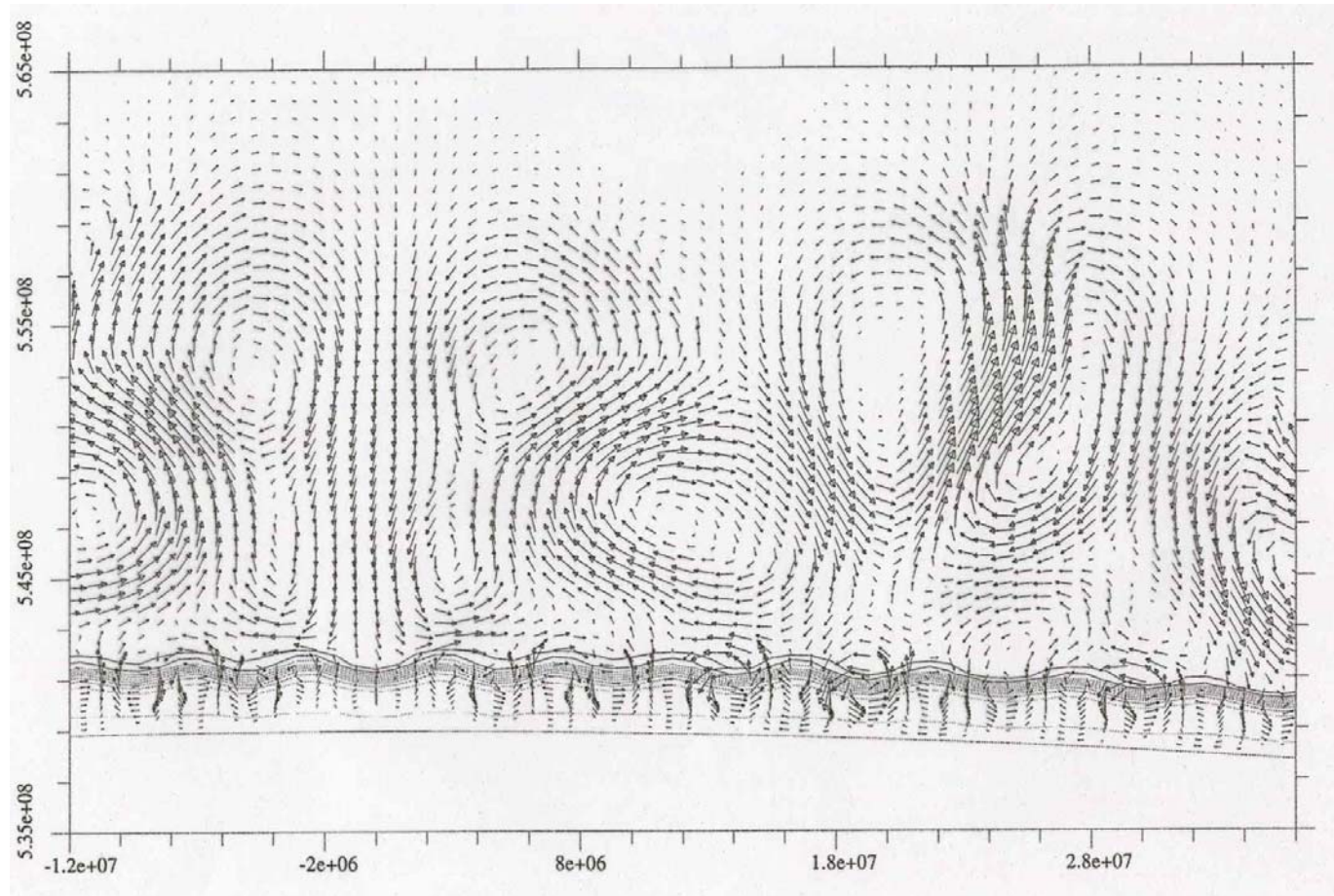
$$V_{\text{late-convection}} \approx 1000 \text{ Km/sec}$$

where $V_{\text{late-convection}}$ is the typical local late convective velocity.

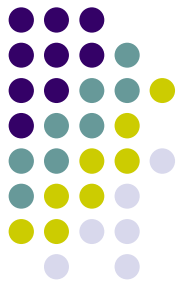
$$V_{\text{sound}} \approx 2000 \text{ Km/sec}$$

where V_{sound} is the typical speed of sound prior to the peak of the runaway.

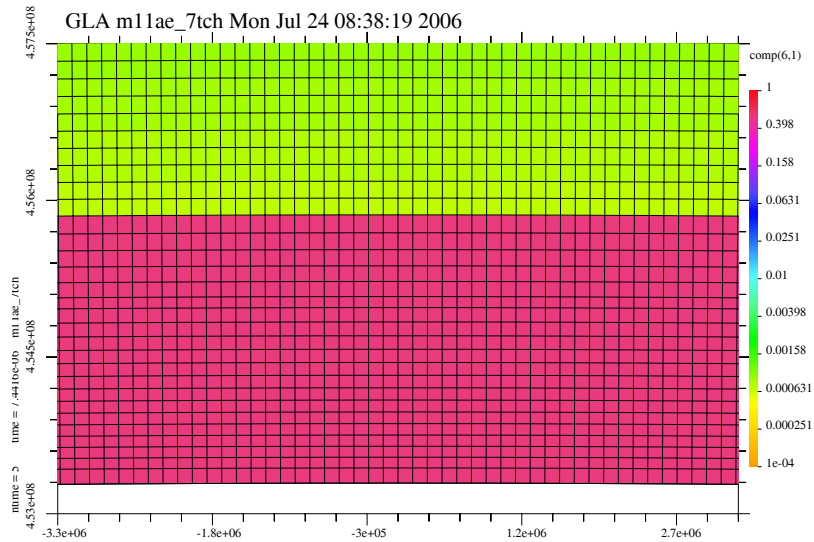
Kelvin – Helmholtz instability lines of equal C(12) abundance



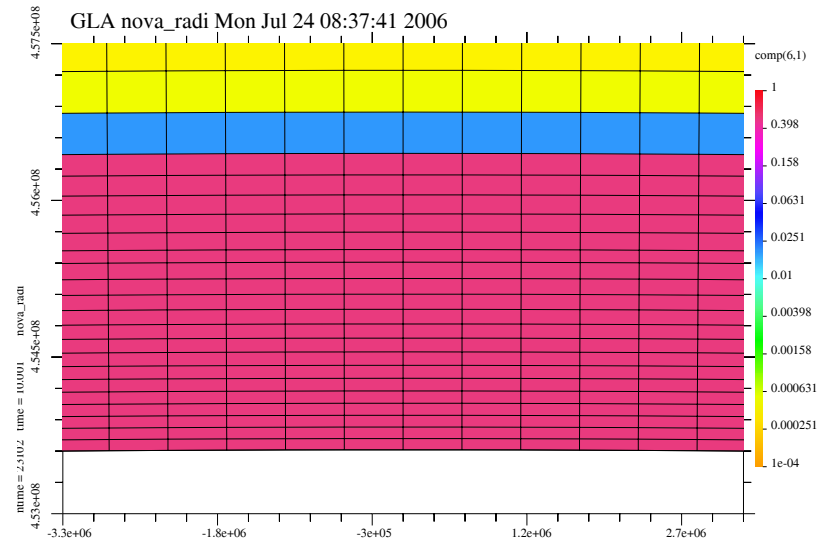
Glasner Livne & Truran 1997 (fig.2)



Improved grid resolution



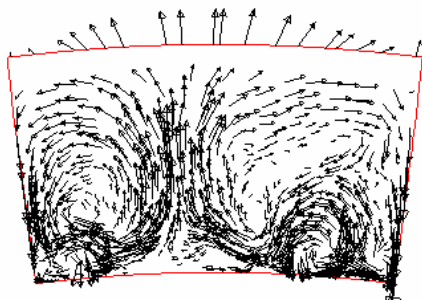
New



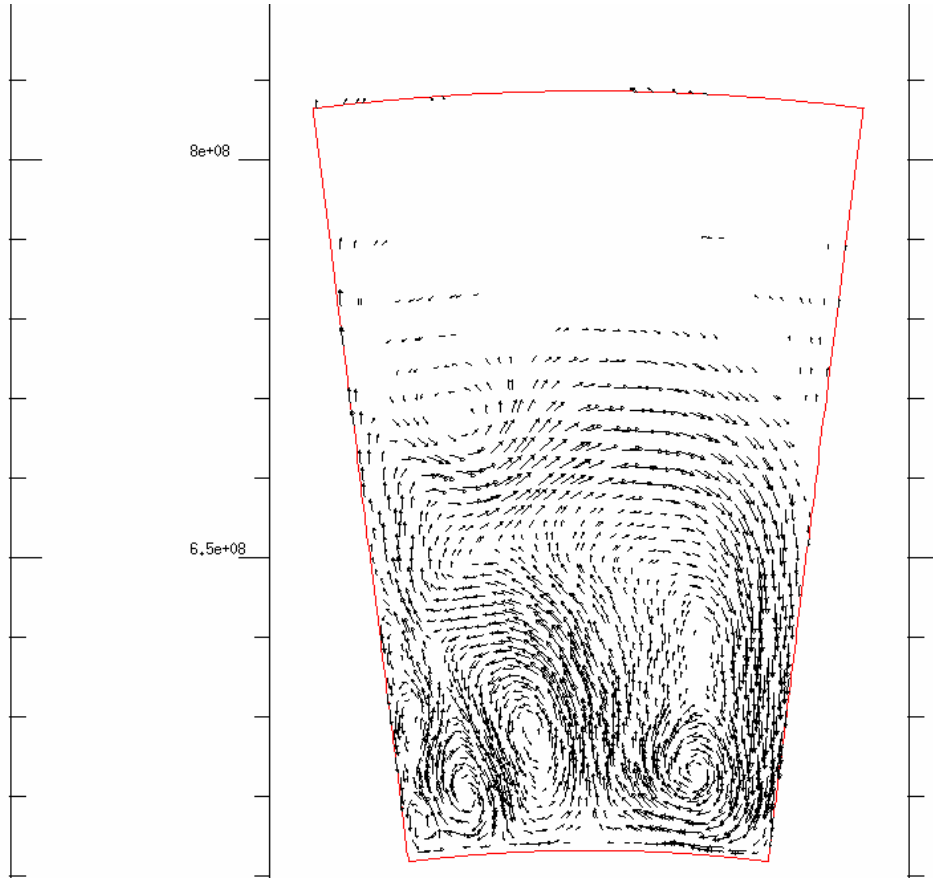
Old

→ Demonstration of the sensitivity
to the outer boundary conditions

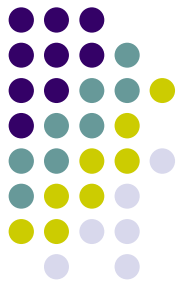
→ The ability to work “Lagrangian”
at the outer zones and “Eulerian”
near the burning regions



Time=130



Time=400



The reference Models

- T7 - Base temperature of $7 \cdot 10^7$ Deg K
- T9 - Base temperature of $9 \cdot 10^7$ Deg K
- T5 and lower → the difficulties.

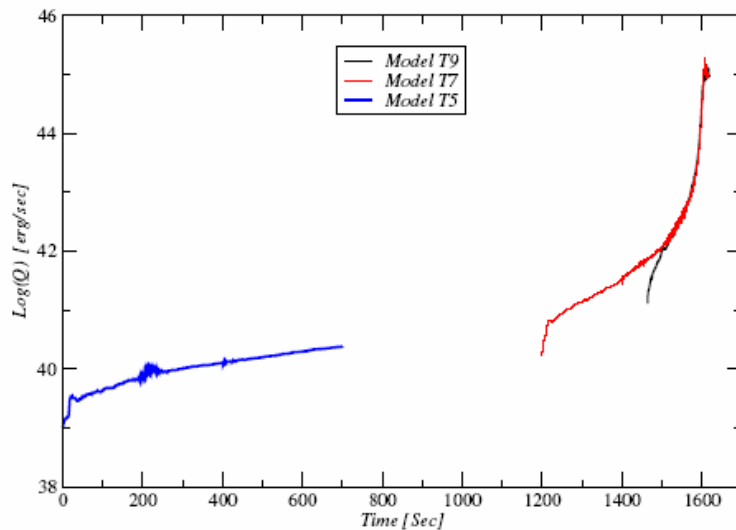
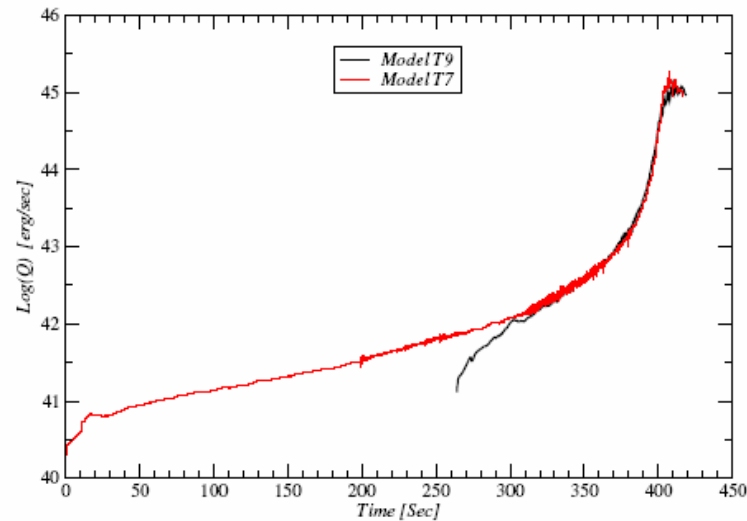
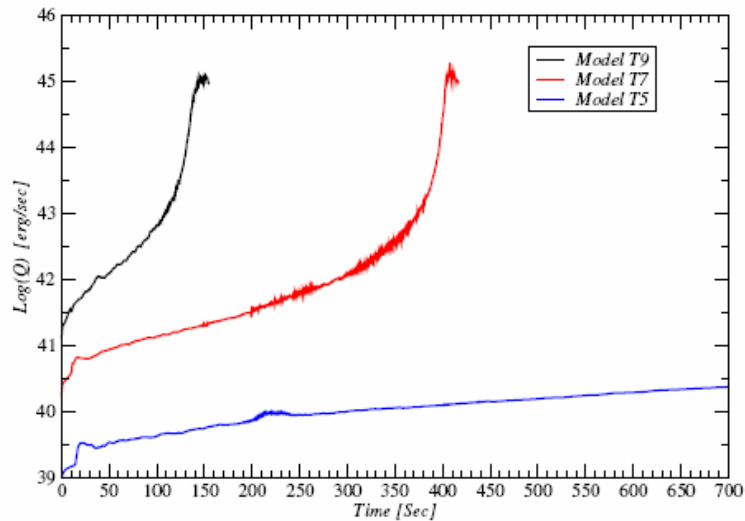


FIG. 3.— The logarithm of the total energy production rate [erg/sec] (Q) as function of time for models T5, T7 and T9 : top-left - nominal times, top-right - the line for model T9 is shifted forward by 264 seconds, bottom - the line for model T9 is shifted forward by 1464 seconds and the line for model T7 by 1200 seconds

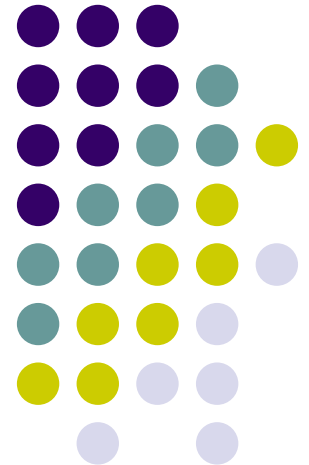
Control Parameter Total Energy Production Rate Q [erg/sec]

Check points:

$\text{Log}(Q)=42,44,45$

At $Q=10^{45}$ erg/sec

Q^* (a few sec)=Binding energy of the
envelope



The overall picture



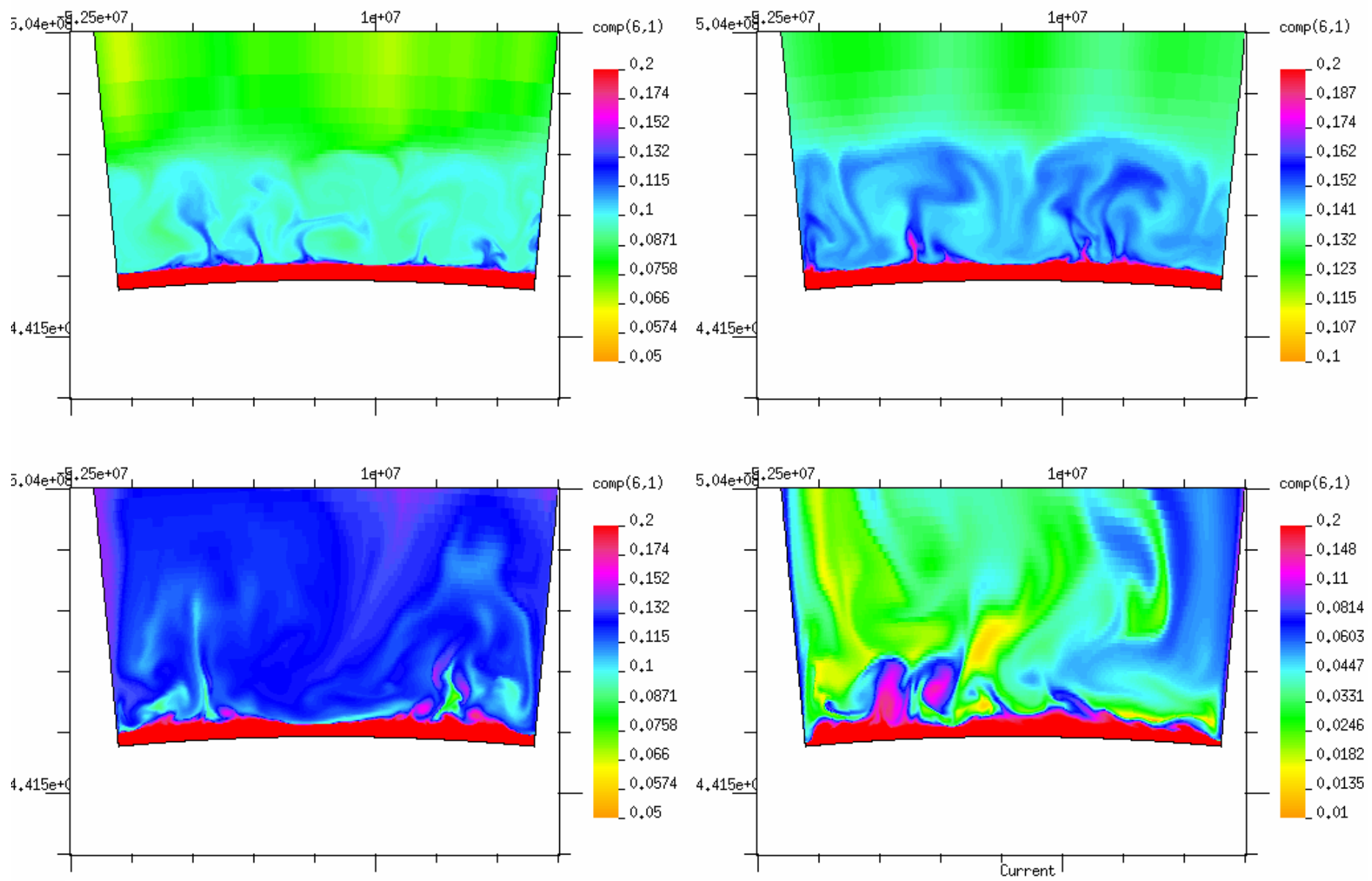


FIG. 1.— C12 abundance for model T7: top left - when $Q = 10^{42}$ erg/sec, top right - when $Q = 10^{43}$ erg/sec, bottom left - when $Q = 10^{44}$ erg/sec, bottom right - $Q = 10^{45}$ erg/sec, note that the colors limit change from one frame to the other

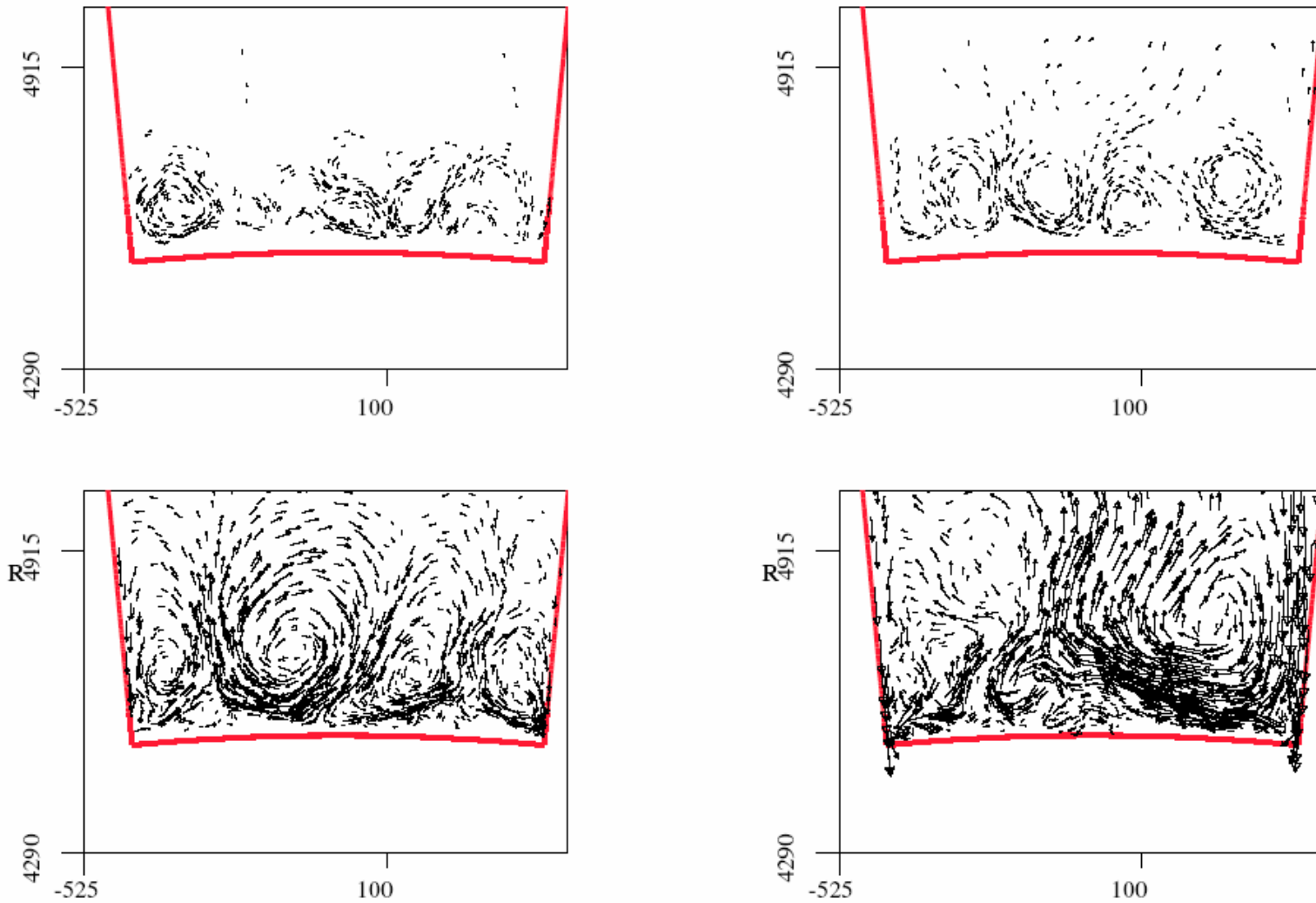
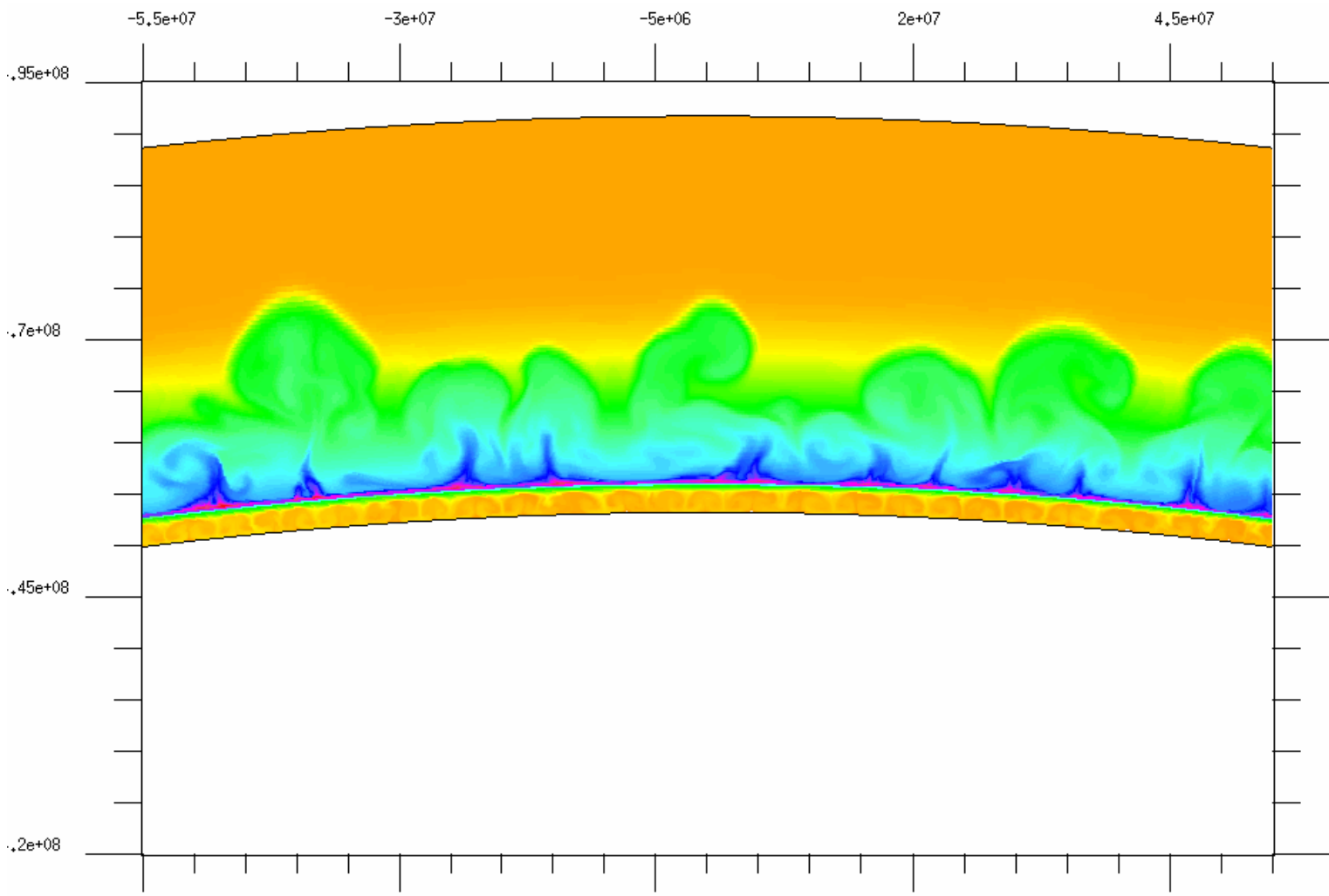
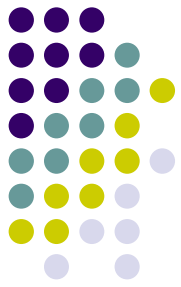


FIG. 2.— Velocity field in model T7: top left - $Q = 10^{42}$ erg/sec, top right - $Q = 10^{43}$ erg/sec, bottom left - $Q = 10^{44}$ erg/sec, bottom right - $Q = 10^{45}$ erg/sec. The velocities are scaled, the highest velocities in the bottom right are about 1000 Km/sec



qreac

The details...



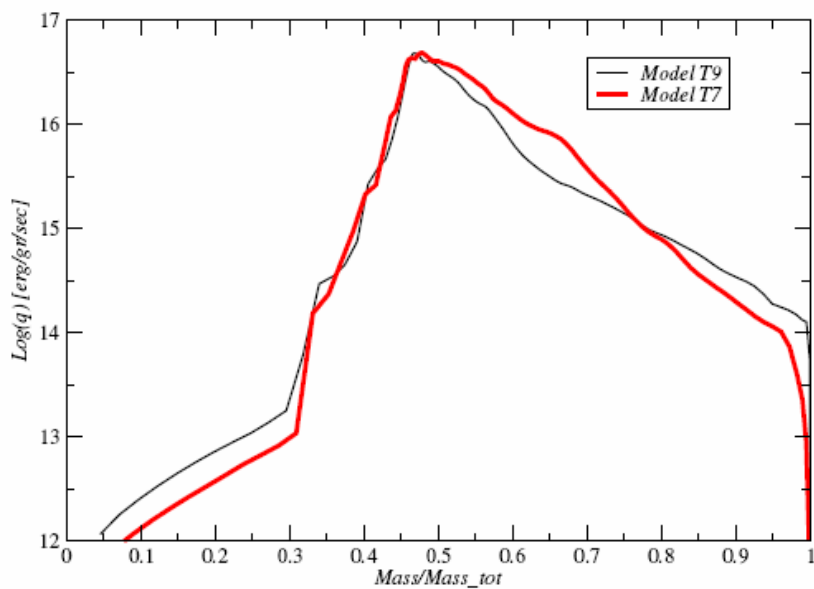
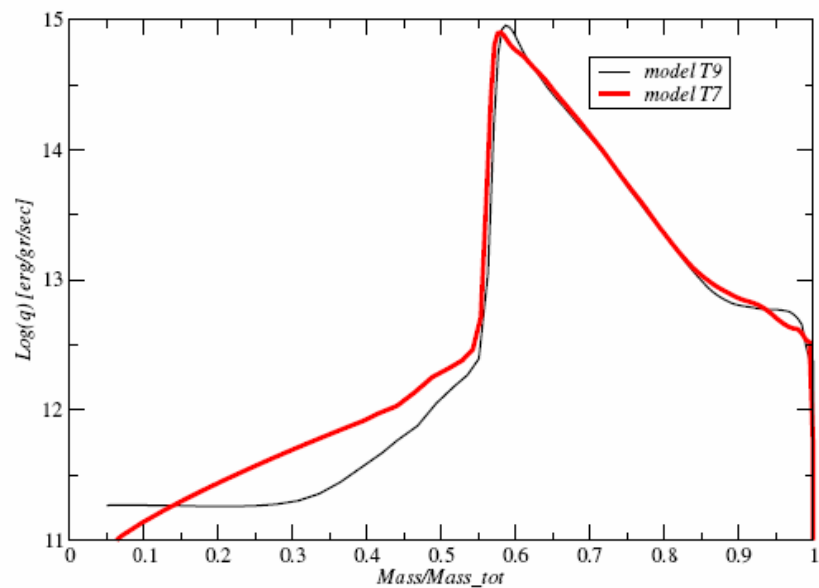
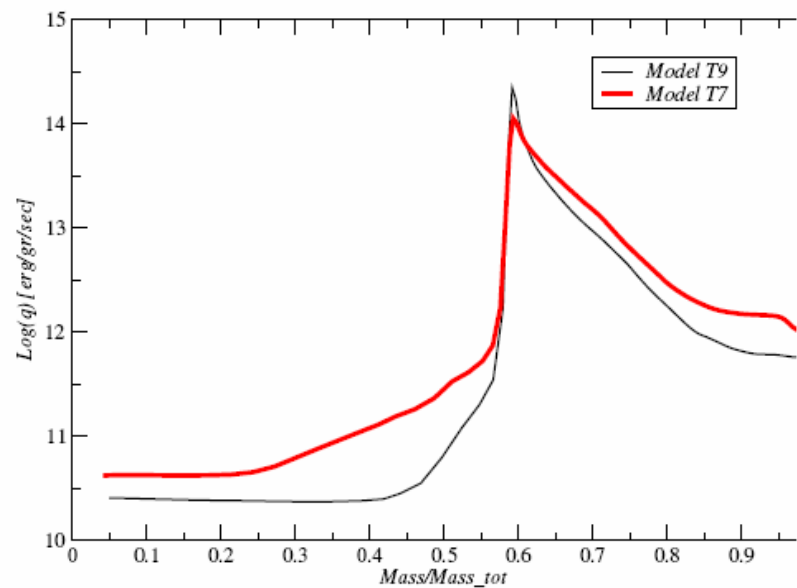


FIG. 5.— Lateral average of Q as function of the fractional mass for models T7 and T9 : top-left - when $Q = 10^{42}$ erg/sec, top-right - when $Q = 10^{42}$ erg/sec, bottom - when $Q = 10^{45}$ erg/sec

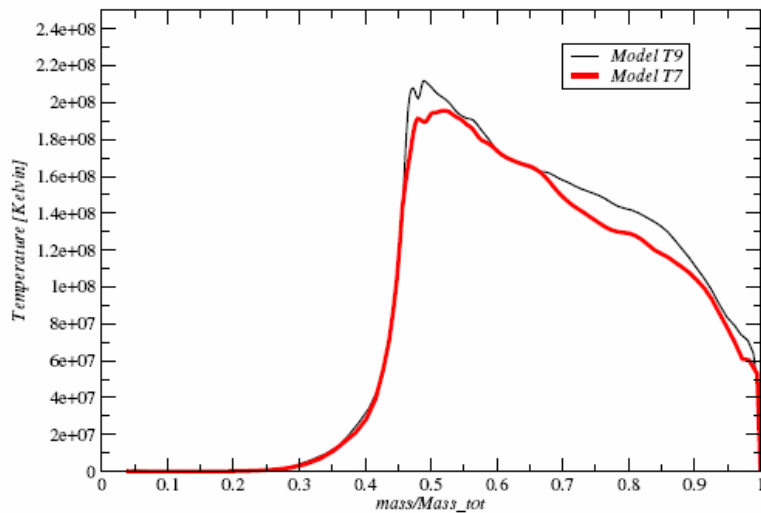
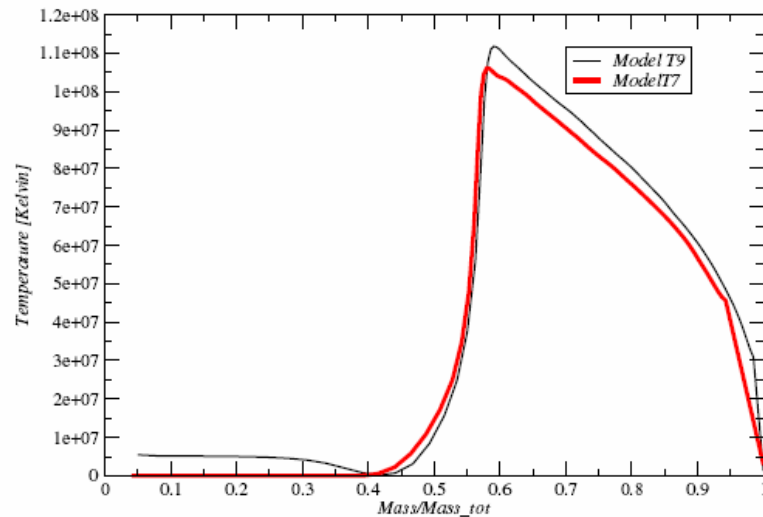
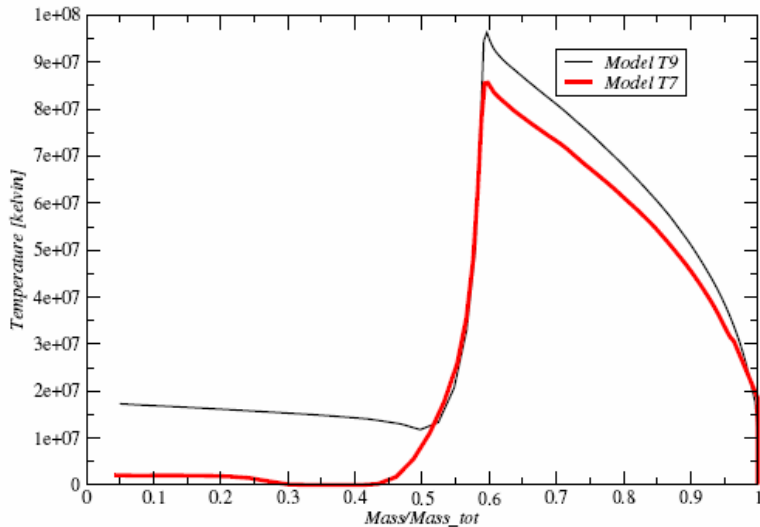


FIG. 4.— Lateral average of the temperature as function of the fractional mass for models T7 and T9 : top-left - when $Q = 10^{42}$ erg/sec, top-right - when $Q = 10^{42}$ erg/sec, bottom - when $Q = 10^{45}$ erg/sec

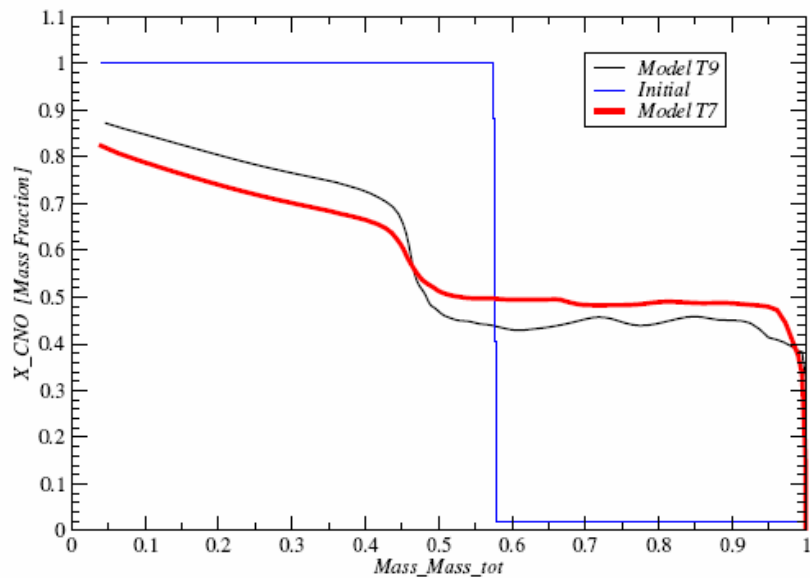
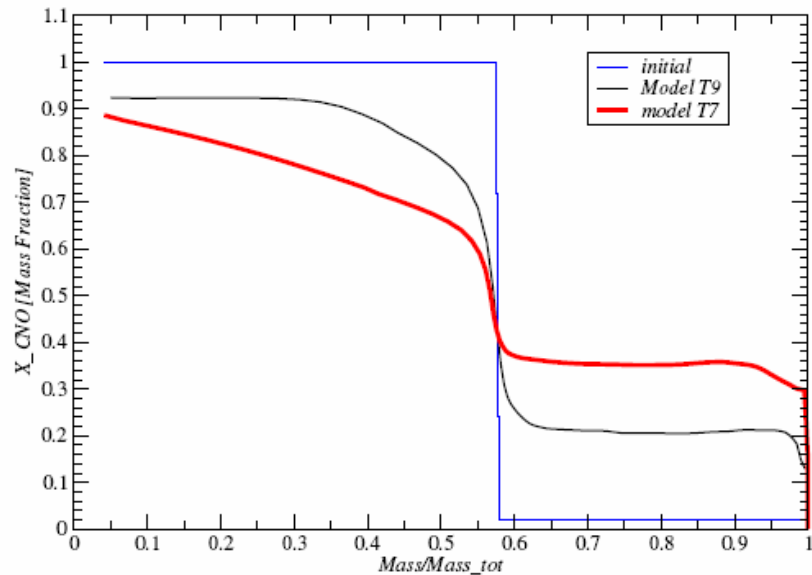
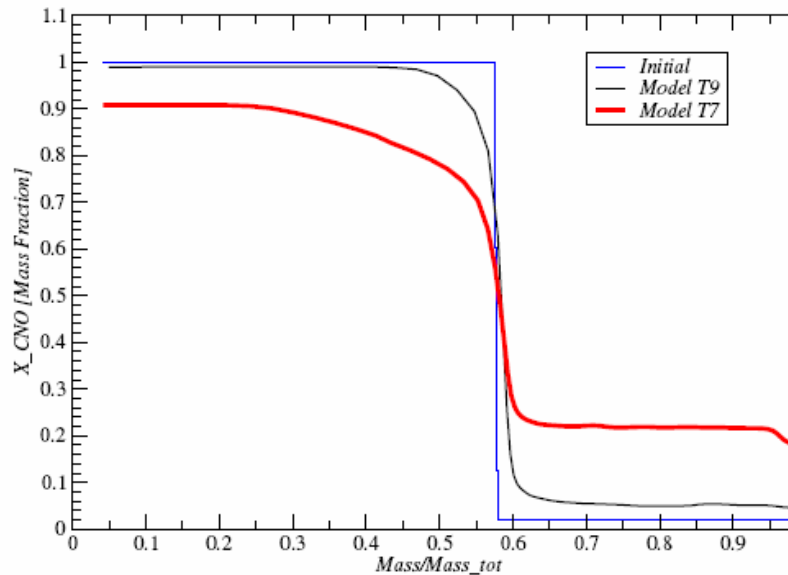
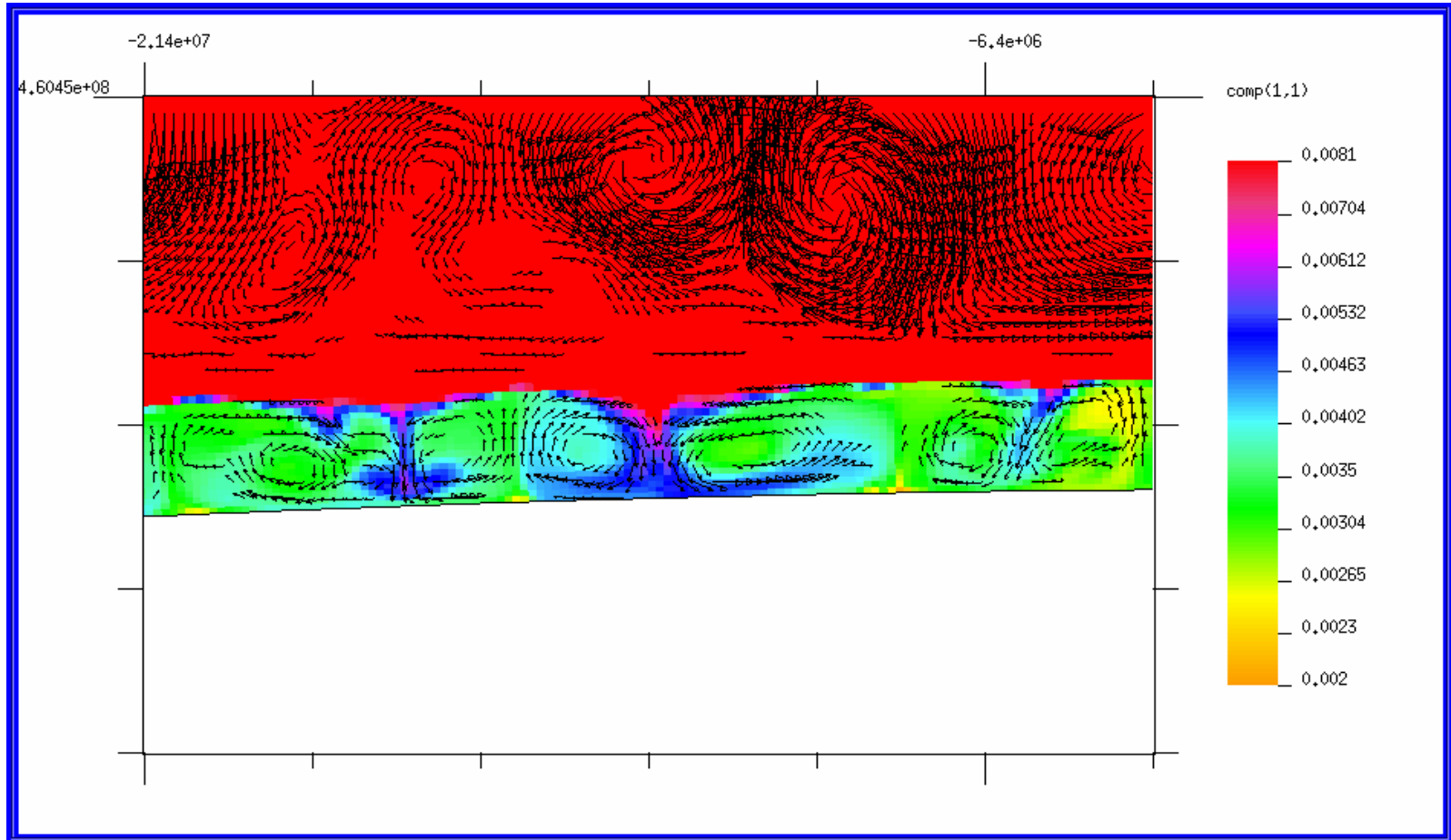


FIG. 6.— Lateral average of the CNO abundance as function of the fractional mass for models T7 and T9 : top-left - when $Q = 10^{42}$ erg/sec, top-right - when $Q = 10^{42}$ erg/sec, bottom - when $Q = 10^{45}$ erg/sec



T=38



Numerical Tests



- Angular range of the grid (same resolution).
- ALE vs. “Effective Lagrangian”

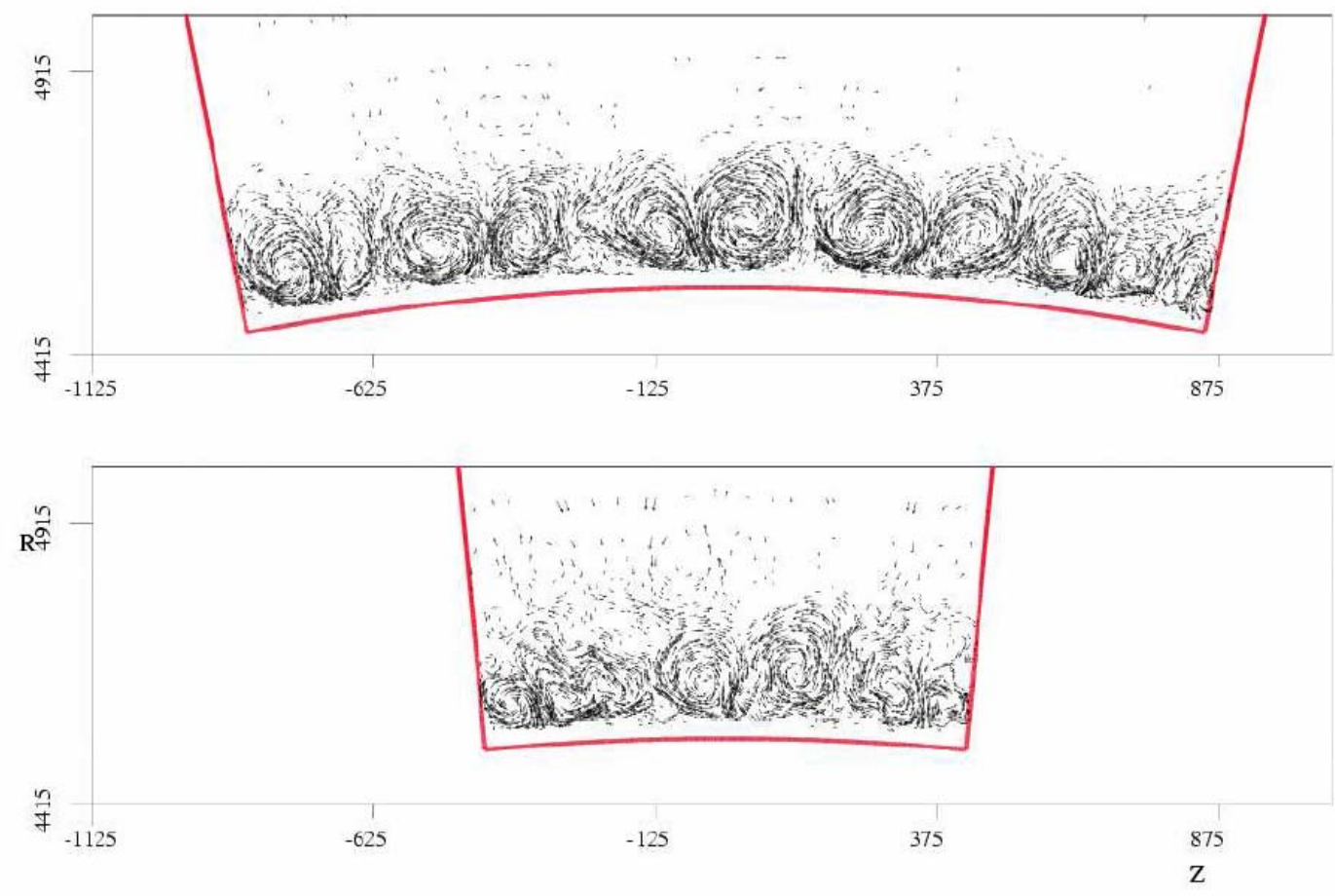


FIG. 9.— Velocity Field of models T7 and $T7_{Wide}$ at $t=300$ sec (R and Z in Km)

Angular dimensions $0.06 \cdot \text{PAI}$ vs. $0.12 \cdot \text{PAI}$

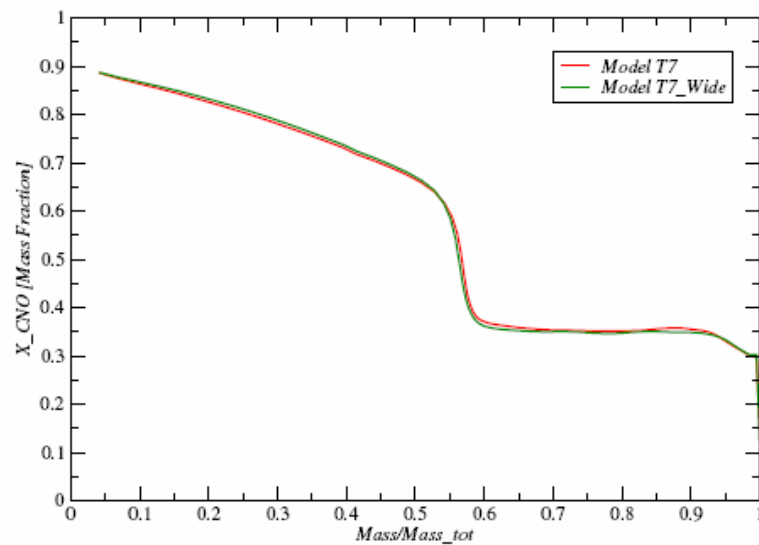
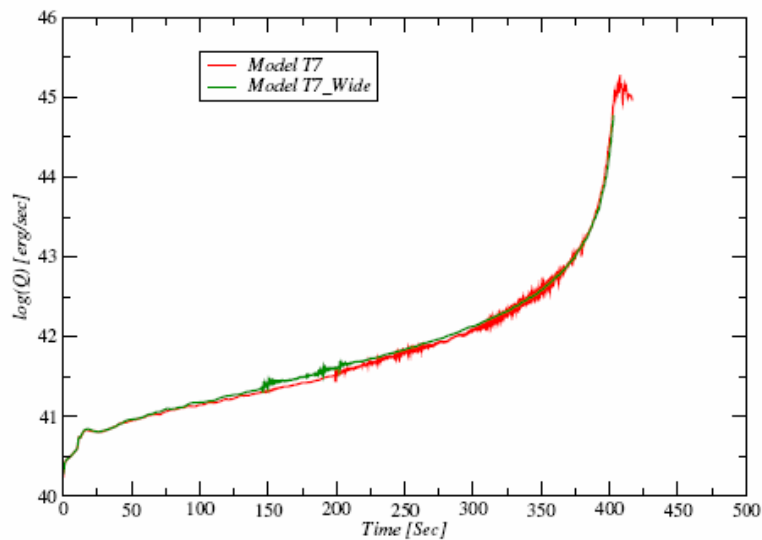
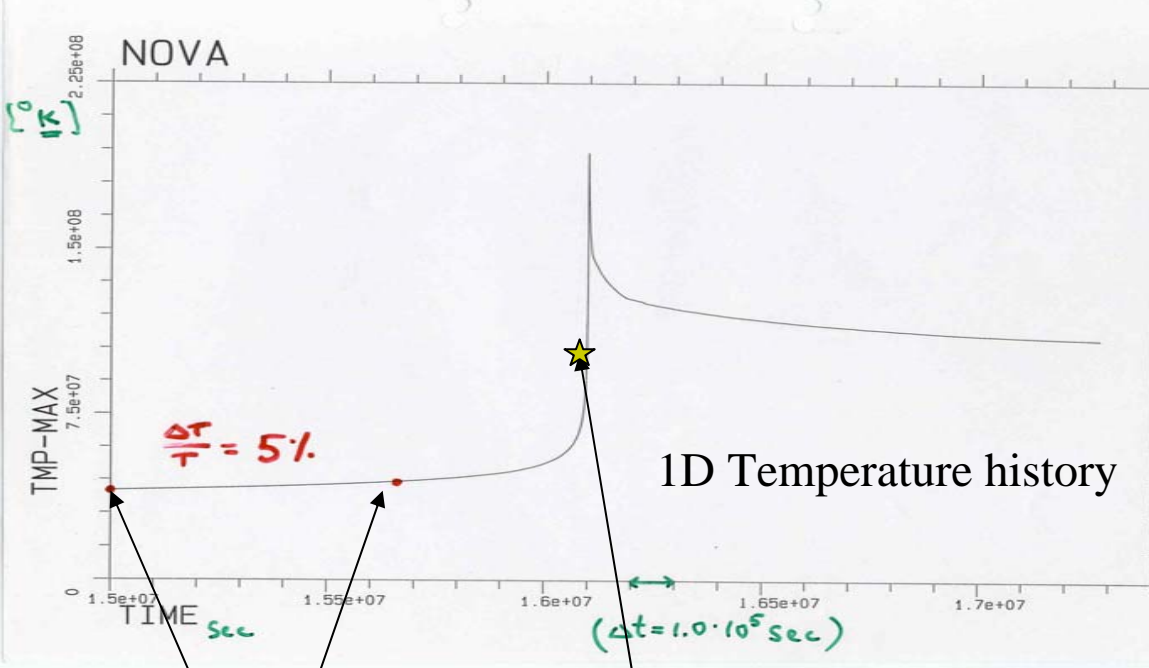
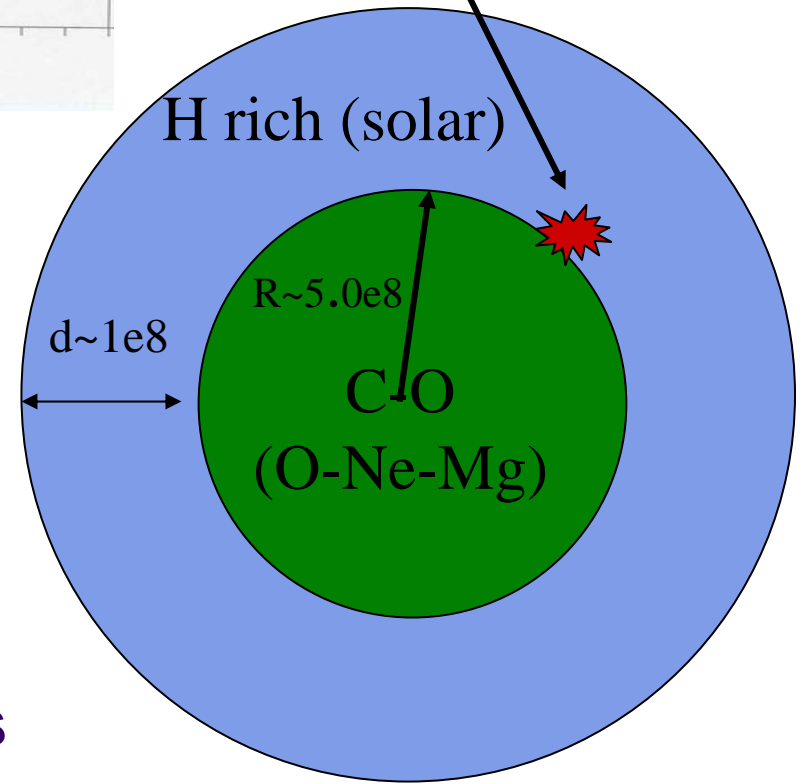


FIG. 8.— Model T7 vs. $T7_{\text{Wide}}$: left - The logarithm of the total energy production rate Q [erg/sec] as function of time [sec] right - The CNO abundance as function of mass when $Q = 10^{43}$ erg/sec.



Local perturbation

Tmp= 10^8 K



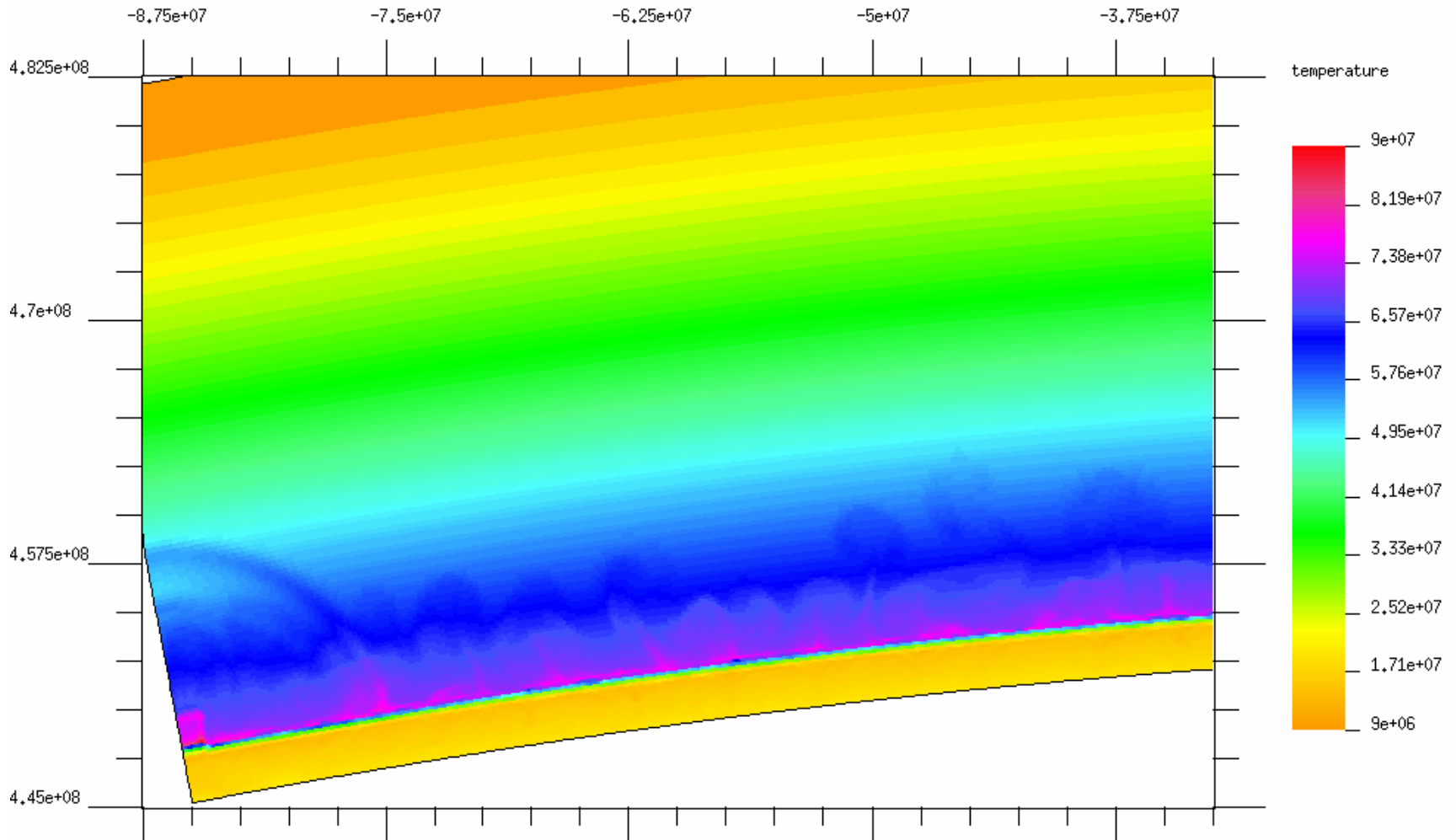
The Fate of Early Perturbations

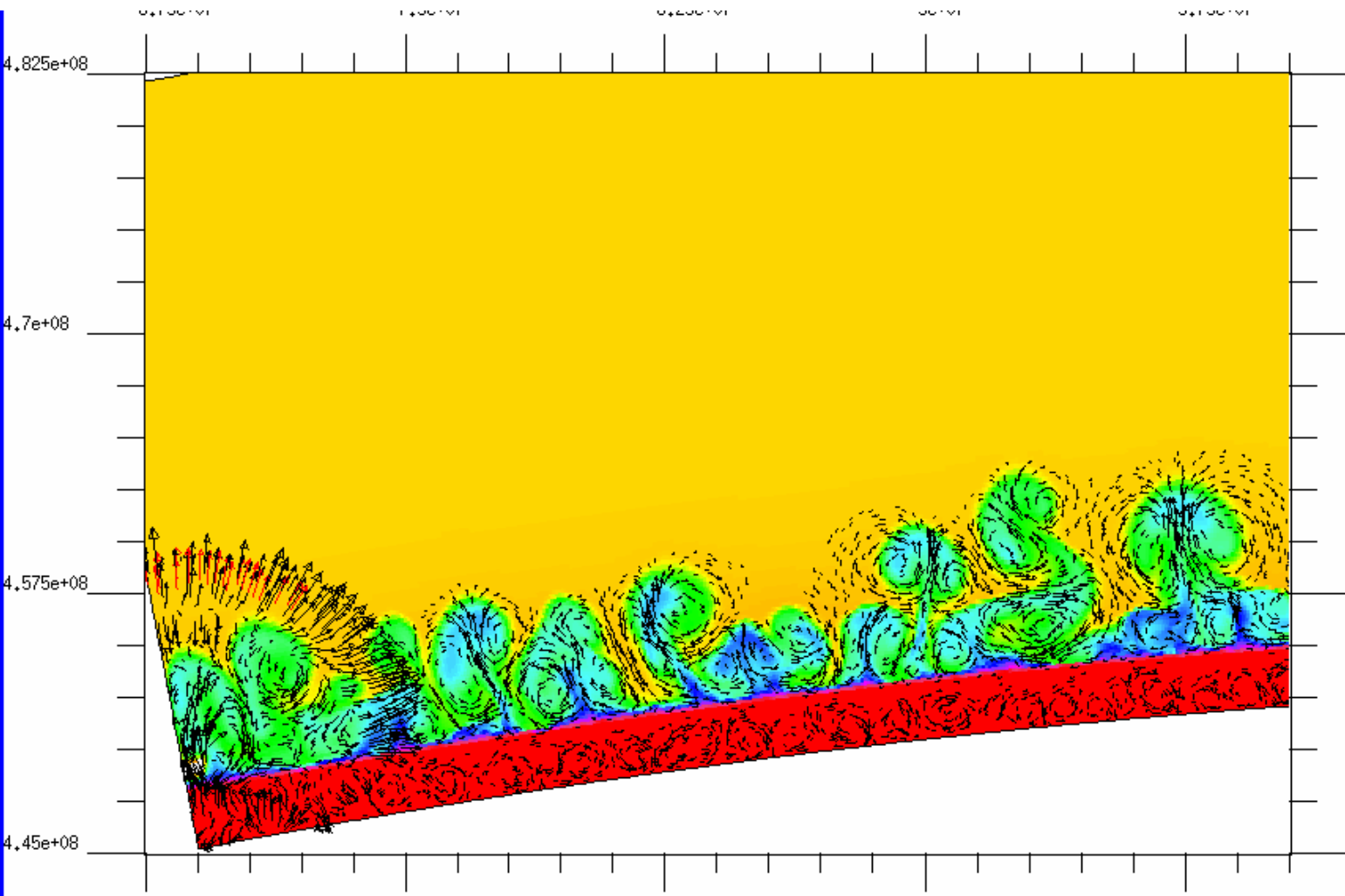
The Fate of Early Perturbations



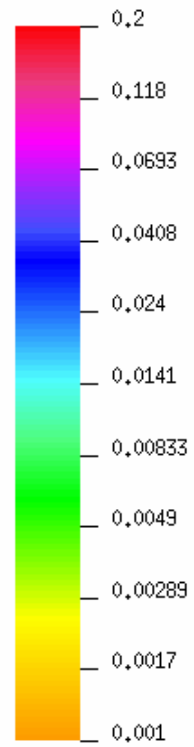
In order to study the consequences of early perturbations the initial model T7 was used as a base line. The model was evolved for 20 seconds in the ALE explicit mode until the convective velocity structures in 2D were fully established. Fluctuations in the convective flow are expected to change the local temperature distribution. The perturbations that are expected to have the largest impact on the flow are those that occur at the base of the envelope and impose also some dredge-up of CO matter from the core. Therefore, at this stage we examine the differences between the evolution, from $t=20$ seconds and on, of the reference case (Model T7) and a model for which we impose a perturbation at the sensitive region defined above (Model $T7_{Perturb}$). The perturbed region includes a significant part of a convective cell and a few zones of the underlying CO core matter ($\Delta R = 7\text{Km}$ and $\Delta Z = 14\text{ Km}$). The abundances of the whole region are fully mixed and the temperature enhanced up to $9 \times 10^7 \text{ }^\circ\text{K}$. The whole procedure was repeated for the wide grid (Model $T7_{Perturb-Wide}$) with its reference model (Model $T7_{Wide}$).

Wide T=20





comp(6,1)



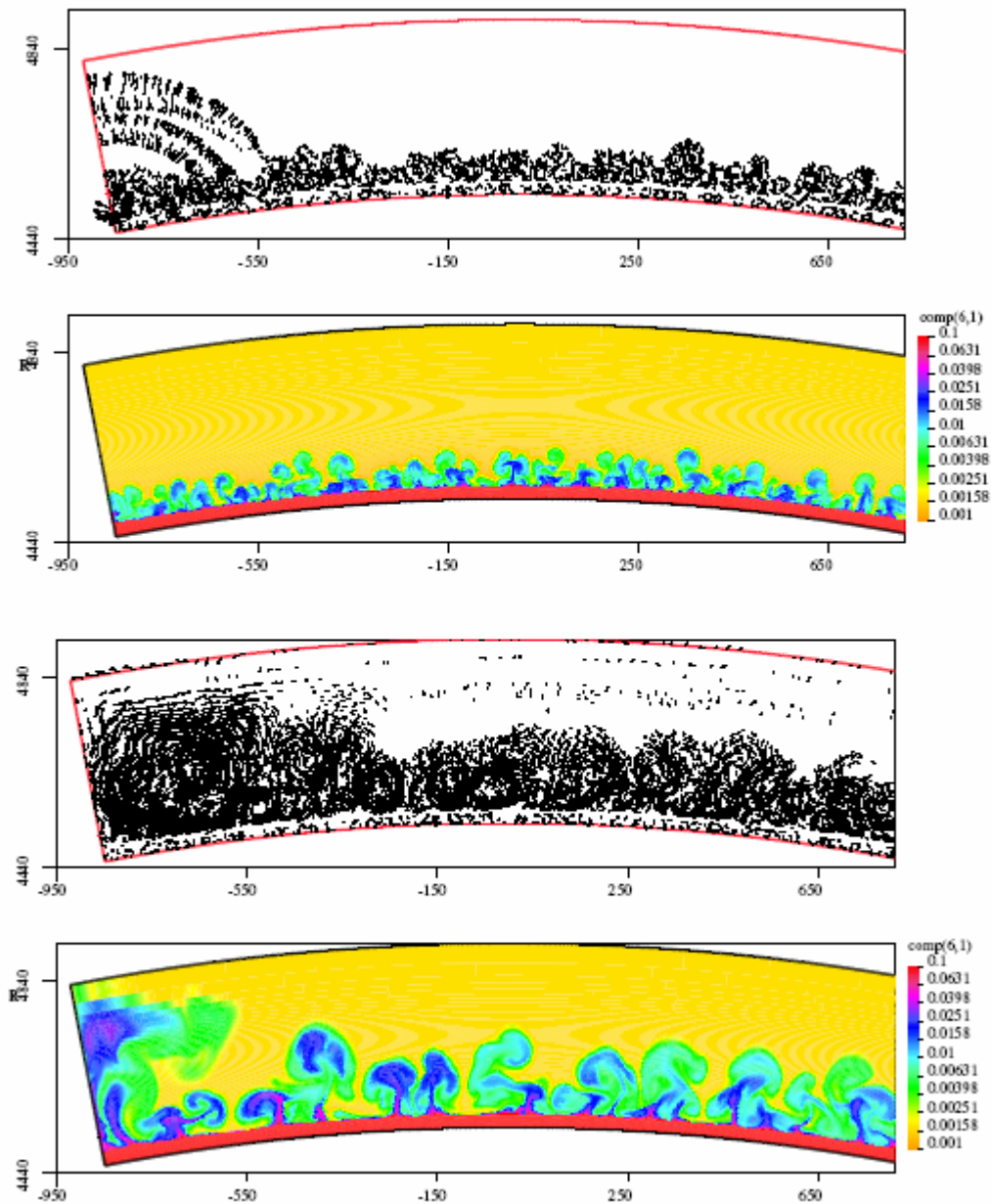


FIG. 12.— Velocity field and C12 abundance for model $T7_{Perturb-Wide}$: top - at time 20 Sec , bottom - at time 26 sec. Velocities are scaled so that the highest velocities are 500 Km/sec

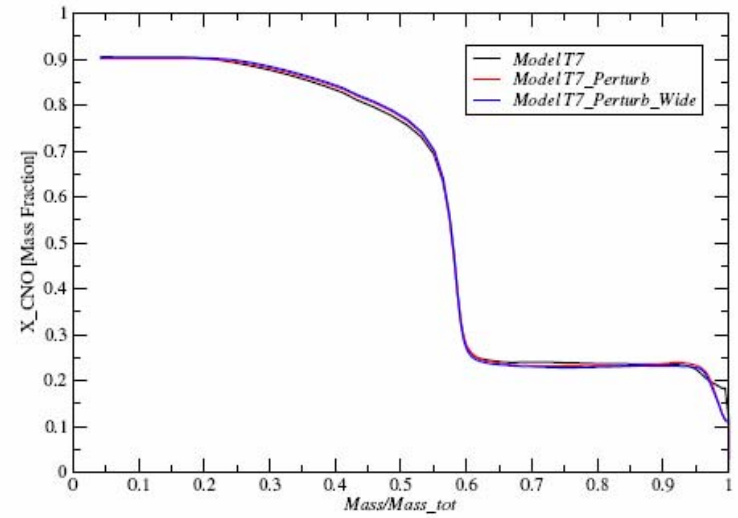
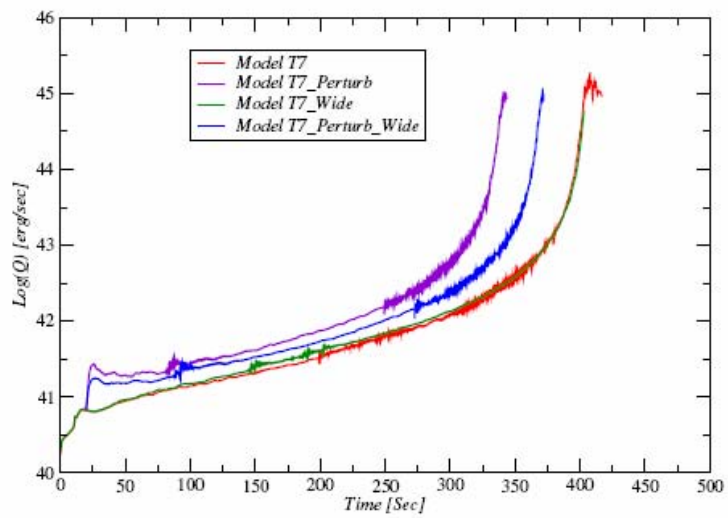


FIG. 11.— models T7, $T7_{\text{Perturb}}$, $T7_{\text{Wide}}$ and $T7_{\text{Perturb-Wide}}$ left - The logarithm of the total energy production rate [erg/sec] as function of time [sec] right - Lateral average of the CNO abundance as function of mass

Special features of the Undershoot Mechanism



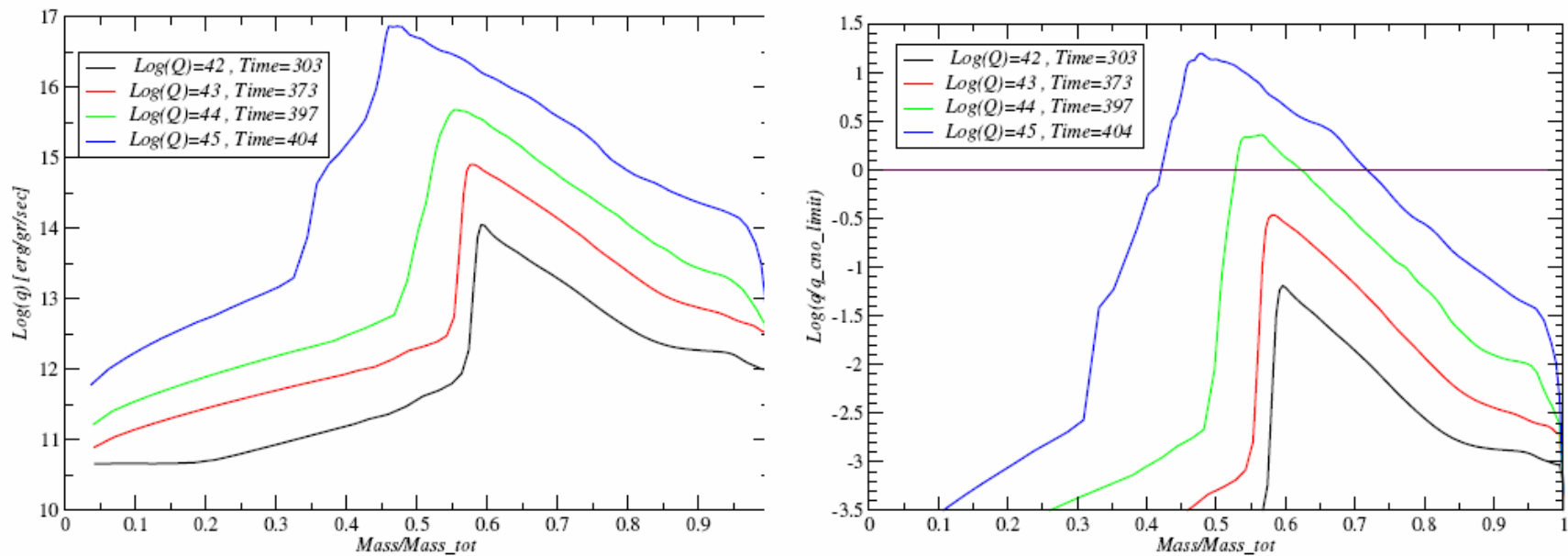



FIG. 7.— model T7 when $Q = 10^{42}$, 10^{43} and 10^{45} left - Lateral average of $\log(q)$ vs. mass ; right - Lateral average of $\log(q/q_{limit})$

$$q_{max} = 5.8 \times 10^{13} \times \left(\frac{Z_{cno}}{0.01}\right) [erg/gr/sec]$$



Discussion

- **Universality Mixing at the level of 30-50 %** 
 - The origin 
 - How far back can we go ? 
- **Mixing**
 - **observations vs. mechanisms**
 - is there a discriminator ?
 - are they all contributing ? Relative importance ?
 - **physical vs. numerical mixing**
 - what else can be done ?
- **Future models ? 3D ?**

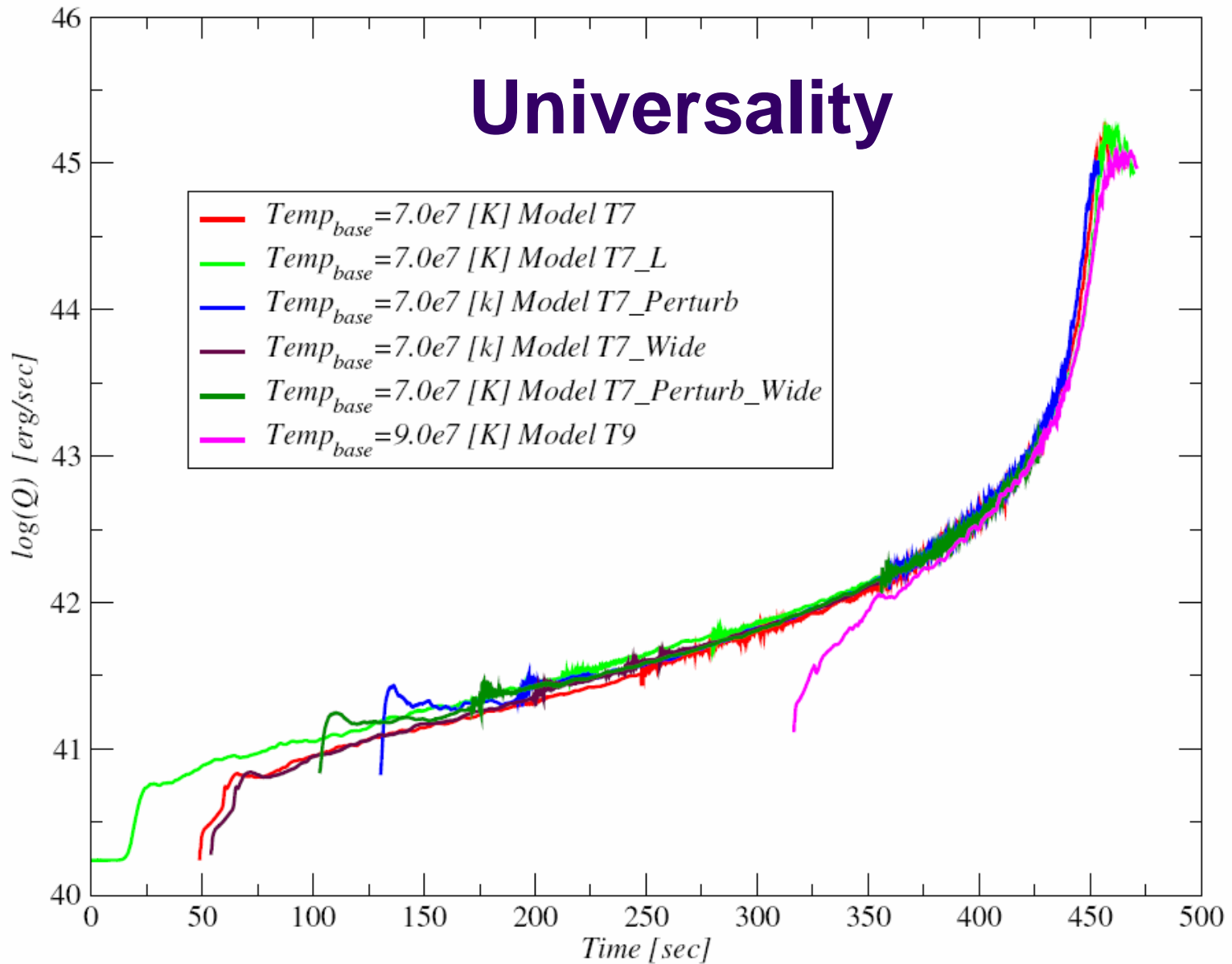


FIG. 15.— The logarithm of the total energy production rate [erg/sec] as function of time [sec] for all the models. The lines were shifted in time in order to show the universality of the models



One Zone Model

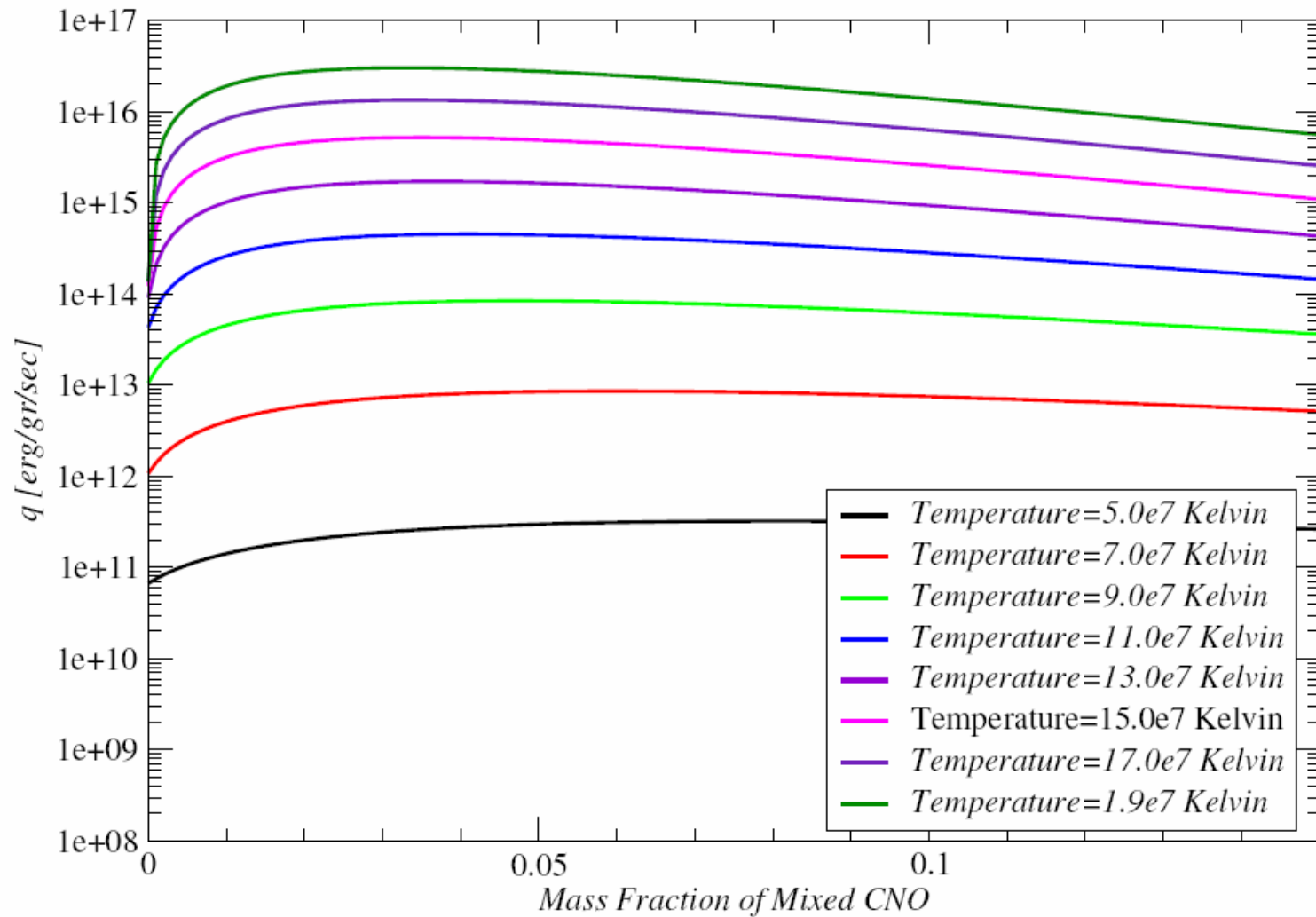


FIG. 13.— Logarithm of the specific burning rates of a mixture of hot solar abundant material and cold CO as function of the fraction of the cold CO for various temperatures.

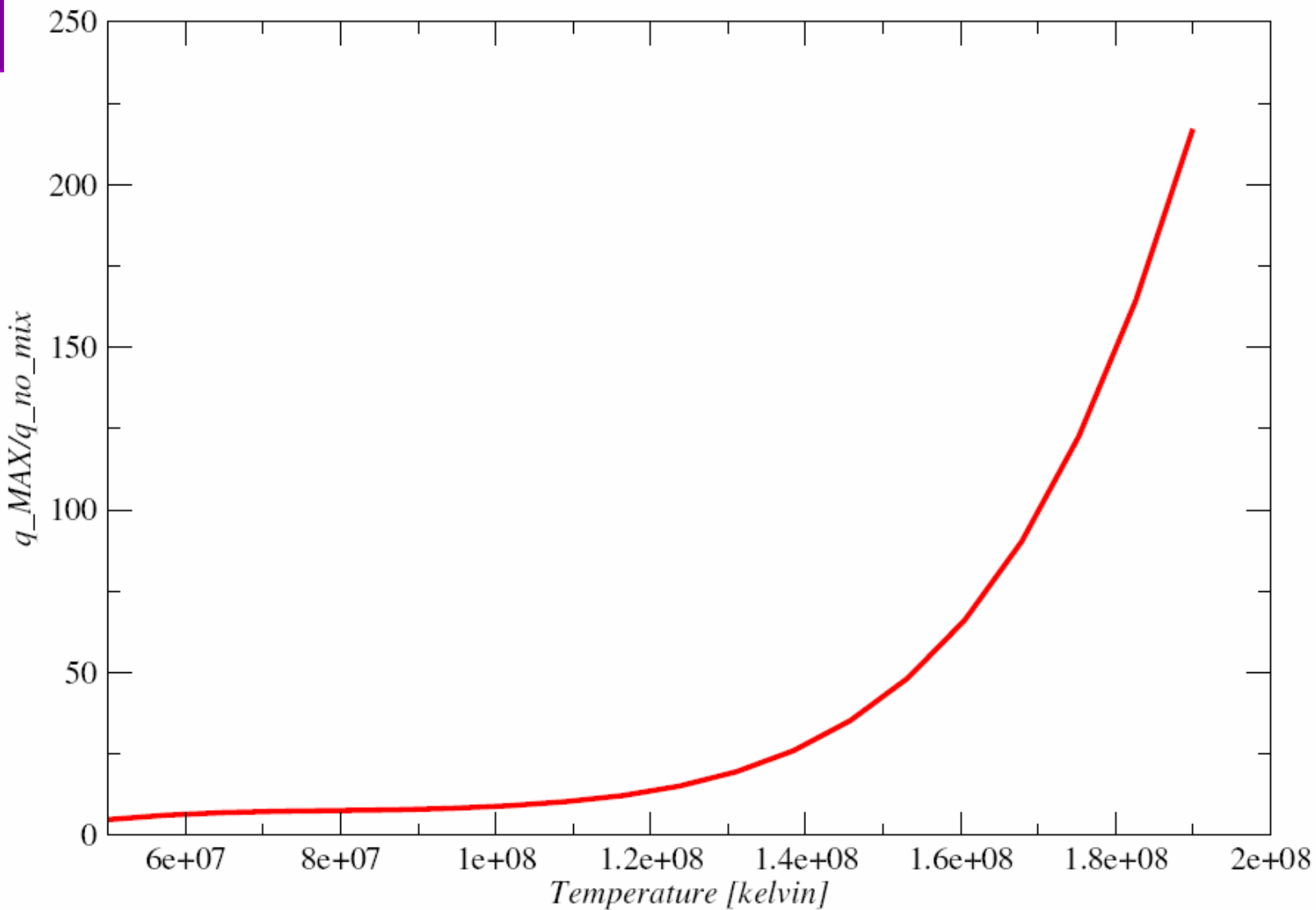
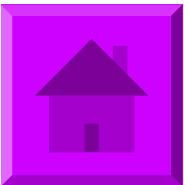
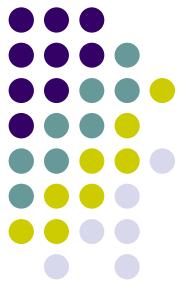


FIG. 14.— The maximal enhancing factor that can be achieved by mixing as function of the temperature of the hot matter.



How far back can we go ?

TABLE 1

TYPICAL EVOLUTIONARY TIMESCALES TO THE RUNAWAY FROM VARIOUS INITIAL TEMPERATURES AT THE BASE OF THE HYDROGEN RICH ENVELOPE. GIVEN FOR: 1D ACCRETING SOLAR, 1D ACCRETING ENRICHED MATER (52.5% H , 12.5% ^{12}C , 12.5% ^{16}O) AND THE 2D MODELS.

NAME	T-base $^{\circ}K$	Δt 1D solar [sec]	Δt 1D enriched [sec]	Δt 2D [sec]	no. of timesteps 2D
T3	3×10^7	1.8×10^8	5.2×10^6	NA	NA
T4	4×10^7	3.8×10^6	1.9×10^5	NA	NA
T5	5×10^7	4.4×10^5	2.2×10^4	≈ 1700	$\approx 7 \times 10^6$
T7	7×10^7	2.6×10^4	2.2×10^3	420	$\approx 2 \times 10^6$
T9	9×10^7	3.2×10^3	8.0×10^2	150	$\approx 6 \times 10^5$

